Titolo della tesi

Effects of a large unsprung mass on the ride comfort of a lightweight fuel-cell urban vehicle

di

Massimiliano Palermo

Tesi proposta per il conseguimento del titolo accademico di
DOTTORE IN INGEGNERIA MECCANICA

presso la
Facoltà di Ingegneria
della Università di Pisa

15 Luglio 2009

Autore:
Massimiliano Palermo .....

Approvata da:
Prof. Massimo Guiggiani .....
Dip. Ingegneria Meccanica, Nucleare e della Produzione
Università di Pisa

Prof. Nick Vaughan .....
Department of Automotive Engineering
Cranfield University

Alla saggezza di mio nonno contadino.

Thesis title

"Effects of a large unsprung mass on the ride comfort of a lightweight fuel-cell urban vehicle".

Abstract

The present thesis work is part of the feasibility study of a lightweight fuel-cell urban vehicle named *Hyrban*. The vehicle mounts four wheel hub electric motors instead of a traditional single motor on the chassis. This causes a sensible increase of the unsprung-to-sprung mass ratio of the car. The aim of the thesis then, has been to investigate the effects of this imbalance, in particular pointing out the attention on the comfort behaviour. Through a frequency analysis of simple models it has been possible to define and evaluate the variation of the comfort index to the mass ratio increase and for various damping coefficients. It yielded not only that the comfort index gets worse as the mass ratio increase, but also that it is less sensitive to its change when the damping coefficient is lower than the optimal value. The last one is variable relatively to the mass ratio, while the total mass and the bounce frequency are assumed to be constant. Other two performance indices have been evaluate about the mass ratio: the suspension working space and the dynamic tyre load. Representing physical limits to the suspension design, as a matter of fact they influence the comfort, even if indirectly. Finally, among various suspension solutions aimed to improve the comfort, only "switchable dampers" are regarded to be a feasible solution for a vehicle with limited amount of space and power.

Titolo tesi

"Conseguenze di una elevata massa non sospesa sul comfort di un veicolo urbano leggero a fuel-cell".

Sommario

Il presente lavoro di tesi rappresenta parte dello studio di fattibilità di un veicolo urbano leggero alimentato a fuel-cell dal nome *Hyrban*. Il veicolo presenta quattro motori elettrici posti sui mozzi ruota anzichè sulla cassa, comportando un netto aumento del rapporto tra massa non sospesa e massa sospesa. Scopo della tesi è stato quello di analizzare gli effetti di questa sproporzione dal punto di vista del comfort di marcia del veicolo. Tramite l'analisi in frequenza di semplici modelli a pochi gradi di libertà si è valutato in particolare un indice di comfort al variare del rapporto tra masse e del coefficiente di smorzamento. Si è concluso che l'indice di comfort degrada all'aumentare del rapporto di massa ma anche che risulta meno sensibile ad esso per valori dello smorzamento inferiori a quello ottimale. Quest'ultimo inoltre, in una logica di massa totale costante e prima frequenza propria fissata, risulta anch'esso variabile rispetto al rapporto di massa. Si sono valutati anche altri indici prestazionali riguardanti lo spazio lavoro della sospensione e la tenuta di strada ovvero la forza di contatto a terra. Essi pongono dei limiti al progetto della sospensione e quindi influenzano, seppur indirettamente il il comfort. Infine, tra varie soluzioni per il miglioramento del comfort, si è ritenuta quella degli "switchable dampers" come l'unica attuabile vista la ridotta disponibilità di spazio e potenza elettrica.

Contents

List of Figures

Chapter 1

Introduction

The present thesis work has been partially carried out in collaboration with the Department of Automotive Engineering of the Cranfield University (UK) within the European students exchange programme 'Socrates' 2006/2007.

In this chapter the background of the project and the motivations that have driven the research are briefly described. Aims and layout of the thesis are also presented.

1.1 Motivation

1.1.1 Alternative vehicles demand

Nowadays automotive market is definitely going towards new scenarios. Traditional cars running only on diesel or petrol internal combustion engines are fated to disappear in next future. During last years all main car manufacturers in the world have started to invest lot amount of money in research and development of non-conventional fuel vehicles. The reasons of this *change of philosophy* are many but they may be easily summarized by two big problems that represent the fundamental issues to cop with:

- Air pollution caused by traditional engines (diesel and petrol)
- Petroleum limited availability (both for natural and political reasons)

European Union have started to face the first problem mentioned introducing a strict legislation regarding emission and consumption standards. All new cars produced have to respect the new directives about emission of carbon dioxide (CO_2) and nitrogen oxides (NO_x). Naturally this measure has brought positive effects like

stimulating the research and development of new technologies addressed to improve the energy efficiency of new engines. Unfortunately millions of old cars are still circulating in Europe and it will take long time to renew all the rolling stock. Besides big new markets are growing very quickly in developing countries like India and China where a modern sensitivity about environmental issues and sustainability is definitely far to come.

The other big reason that leaded, and will lead, to important changes in cars propulsion technology is the limited availability of oil on the planet. Naturally petroleum reserves are not infinite and are destined to run out sooner or later being not renewable. A shorter term problem, but not less difficult to resolve, is the effective accessibility of this reserves seems to be. As a matter of fact the aggressive political strategies carried out during last years for the control of areas rich of petroleum reserves, or the speculative economic behavior of the association of producing countries (OPEC), demonstrate how important and crucial is the argument, not only for the automotive industry but especially for the whole energy supplying division yet strongly dependent from fossil fuels.

Despite some practical realizations of non-conventional fuel vehicles dates back many years (e.g. LPG vehicles, solar, etc.), they have never represented, for several reasons, a real alternative to traditional fuel as diesel and petrol. According with the motivations exposed above, it is also probable a re-discovery and improvement of these experimented technologies in parallel with the efforts towards brand-new solutions (e.g. fuel cells, plug-in electric vehicles, etc.).

A detailed description of different typologies and characteristic of all existing alternative fuels (intended here as not deriving from petroleum) is naturally out of the aims of this dissertation. Although in order to understand the contest which the present work is placed in, a partial list of the most relevant solutions is presented. A rough subdivision of non-conventional fuel cars may be done as follow:

1. Single fuel source:

- Hydrogen vehicles:
  - Hydrogen internal combustion engines;
  - Fuel cells with electric motor drives.
- Battery Electric Vehicles (BEVs);
- Bio-fuels vehicles;
- Compressed Natural Gas vehicles (CNG).

2. Multiple fuel source:

- Hybrid vehicles:
  - Hybrid Electric Vehicles (HEVs);
  - Plug-in Electric Vehicles (PHEVs).
- Flexible fuel vehicles.

Among the previous solutions electricity and hydrogen fuels based vehicles have the big advantage of an high flexibility with respect of primary energy sources, with the possibility to select from various renewable energy sources. According to this it becomes clearer how HEVs and hydrogen vehicles represent the most valid alternatives to traditional cars.[1]

Hydrogen vehicles, instead, are a newest technology compared to standard hybrids. A first, and relatively simpler application, has been the use of hydrogen gas, pure or mixed with other gases (usually *methane*) to be burned in standard petrol engines.[2] A longer term application, which still needs to be efficiently developed for a commercial use, is the use of fuel cells propelled by hydrogen gas stored in cylindric tanks. Inside the cells an electrochemical reaction permits to obtain electric energy ready to be used directly to power electric drive motors or either stored in batteries.

1.1.2 The *Hyrban* project

The present work is part of a main project named *Hyrban*, which intends to fulfill the requirements and the considerations made above.[3] The project has born from the collaboration of several UK partners, both from academic and industrial world: Cranfield University, Oxford University, BOC Foundation and OSCar Automotive Ltd. *Hyrban* project has the objective to design and develop a **two-seat hydrogen fuel-cell vehicle for urban application.** The project aims to prove that practical urban vehicles can be engineered using existing fuel-cell technology. Among many alternative solutions it has been chosen to follow some technical guidelines that represent the philosophy which the project is based on.
The main characteristics of *Hyrban* car be summarized as follow:

In-wheel electric motors. Powered by the electricity created inside the fuel cells, they represents the only drive system of the car. The use of electric motors

[1] A detailed description of strengths and weaknesses of the various systems is available in [5].
[2] A well known example is the BMW *Hydrogen 7* developed on the basis of a commercial sedan.
[3] A complete argumentation about reasons and tenets at the basis of *Hyrban* project can be found in [13].

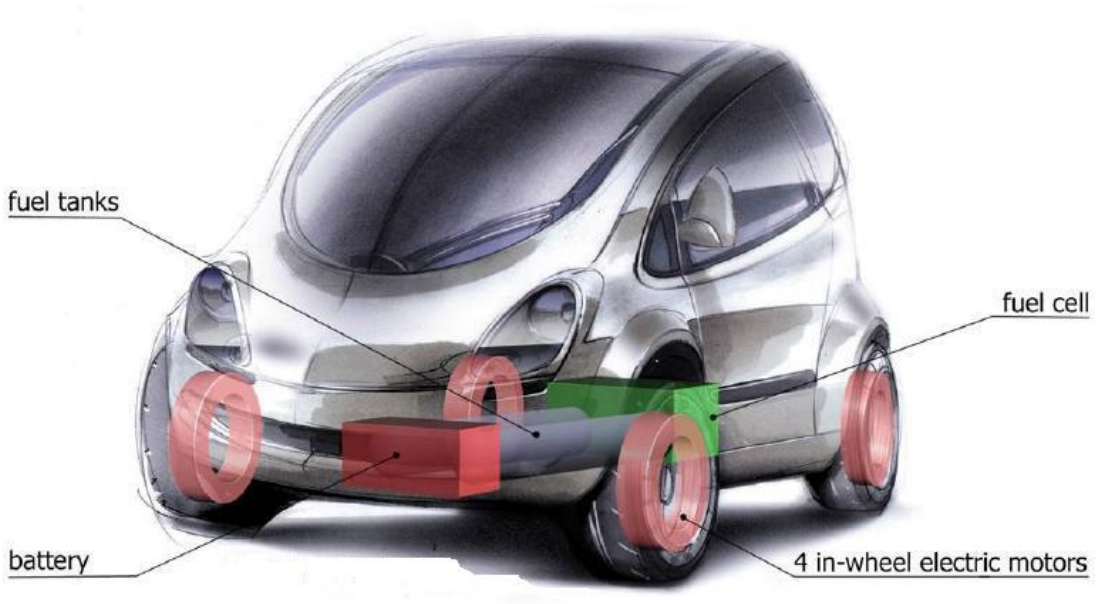

Figure 1.1 – Illustration of *Hyrban* car characteristics.

directly fitted inside the hub of the wheels permits to avoid any other transmission devices (e.g. gears, joints, etc.) with clear advantages in terms of energy efficiency.[4]

Lightweight strut. This specification constitutes the most important demand in order to achieve levels of acceleration comparable with those of a Smart Car. Thus the design needs to be pointed both to reduce the absolute number of particulars composing the car, and to reduci the weight of them (e.g. fibreglass body, aluminium chassis, etc.).

Regenerative braking. Most of the braking power required is supplied by the same electric in-wheel motors that, during braking and release phases, work as generators recharging a group of ultracapitors present on the vehicle. Traditional brakes are also present but they have essentially a safety role and they can be under-designed.

In Fig. 1.1[5] the typology of the vehicle studied and his technical characteristics are schematically showed.

The presence of the regenerative braking puts the attention of the *Hyrban* powertrain system. It is very different from a conventional linear powertrain, being more

[4]Pro and contra of this choice will be further discussed in § 2.1

[5]The drawing refers to SMEH, a Slovenian project having many peculiarities in common with the *Hyrban* project.

properly defined as a "network electric powertrain". A sketch of the energy flow for each phase (cruising,accelerating and braking/release)is showed in Fig. 1.2. As said above, apart from the fuel-cell, there are a group of ultracapacitors. Their presence is fundamental in order to provide the necessary additional power for acceleration. In fact the constant-level (*cruise*) power demand is decoupled from the acceleration demand. Fuel cells provide only the modest power necessary to cruise (almost five-fold smaller than acceleration demand) and for this reason they can be lighter and less powerful. On the other side the ultracapacitors work as a battery storing the energy saved during the regenerative braking phase. The energy stored is released during acceleration phase when a bigger amount of power is required. In this way the four electric motors needs to be connected with both the ultracapacitors and the fuel-cell. In Fig. 1.2 it is also showed how in a traditional system without re-generative braking the energy is lost in form of thermal heat from the brakes discs. Besides it is necessary the presence of transmission systems with consequent further loses in terms of efficiency.

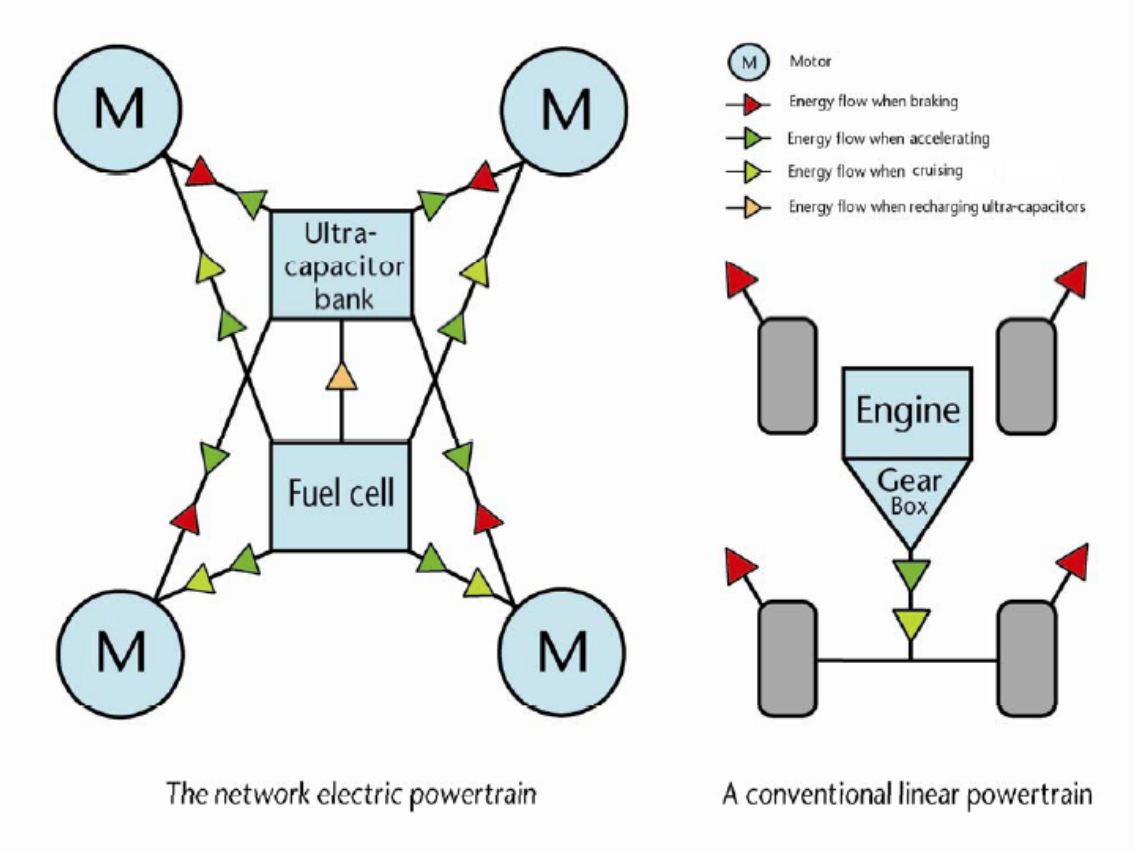

Figure 1.2 – Comparison between Hyrban network powertrain and a conventional one.

Several feasibility studies have been conducted on each different subsystem of the project (fuel cells, suspension system, chassis design, drive system, etc.). Their design is clearly inter-connected having to deal with all the technical bonds and restrictions present in the other subsystems.

1.1.3 Problem statement

Within the feasibility study methodology described above, the present work represents a section of the design and optimization of the suspension system addressed to the improvement of the Ride quality of the *Hyrban* car.

An important parameter influencing the dynamic behaviour of a vehicle is represented by the **unsprung-to-sprung mass ratio (μ)**. It is defined as the ratio between the "not suspended" mass of a vehicle (e.g. wheels, tyres, part of suspensions structure, eventually brakes, etc.) called *unsprung mass* m_u, and the remaining part of the mass supported instead by the suspension (e.g. chassis, engine, passengers, etc.) called *sprung mass* m_s. The value of the mass ratio μ is affecting both the vertical and the lateral dynamics (*ride* and *handling*) of a vehicle. In fact the passenger comfort level and the road holding performances are strongly dependent on the value of μ.

The particular drive system of the *Hyrban* car causes a shift of the mass distribution in the vehicle from sprung to unsprung mass. While the weight of the electric motors and the presence of regenerative brakes make the unsprung mass m_u increase, the absence of a traditional transmission system and the lightness of the composite material used for the body make the sprung mass m_s decrease.

The high value of the unsprung to sprung mass ratio μ of the *Hyrban* car is the motivation of the present work. The reasons why this argument represents an issue to be investigated may be summarized as follow:

- The majority of the commercial vehicle in use have a mass ratio approximately of $\mu = 0.1$ ($m_s \approx 10\ m_u$). This value is considerably lower than the mass ratio of the *Hyrban* car ($0.15 \leq \mu_{\text{Hyrban}} \leq 0.35$). A low mass ratio is commonly considered preferable for both comfort and road holding requirements. A prove of that are the big efforts made from all the car manufacturers and designers to reduce the unsprung mass with solutions like the use of mag wheels or independent suspension systems;

- In technical literature several sensitivity studies about the effects of the variation of the mass ratio in a vehicle has been done but all of them stand beyond

the hypothesis that $m_u \ll m_s$, hypothesis clearly not applicable at the case of the *Hyrban* car. Besides previous studies consider the sprung mass as constant when mass ratio increases, while in this case it is the total mass to be constant;

- In high level cars many different strategies have been studied and adopted to improve the quality the ride comfort (e.g. active suspension, multi-link suspension, etc.). But the range of possible solutions is strongly reduced by the nature of the *Hyrban* project. In fact firstly the *Hyrban* car is a lightweight vehicle with all the limitation peculiar of small urban cars. Furtherly, as said in the previous section, there are several technical limitations about space and energy available that make most of the traditional solutions to be inapplicable (or out of the setting range) for the *Hyrban* car, making necessary the development of new strategies;

An accurate comprehension of the nature of the problem has been then necessary in order to approach a valid ride improvement strategy and to make some recommendations about design and setting of the suspension primary elements (springs and shock absorbers).

1.2 Aims and objectives

According to the motivations exposed, the *aims* of the present thesis are:

1. **to study the effects of a large unsprung-to-sprung mass ratio on the ride comfort of a lightweight fuel-cell vehicle for urban application.**
2. **to investigate solutions and evaluate possible strategies to reduce negative effects.**

In order to reach the general aims it has been necessary to fulfill and pass through the following specific *objectives*:

- development of Matlab vehicle models to evaluate the effects of a large mass ratio on ride behaviour.
- first choice of *primary ride* parameters (springs and shock absorbers) according to ride quality evaluation.
- determination, among several options, of a suspension strategy to adopt for future optimization.

1.3 Thesis layout

The second chapter present all the background that has been necessary to the present study as road profile random characterization, vehicle vibration analysis and suspension strategies. Most of the mathematical definitions and known literature results used are described in this chapter.

The third chapter is relative to the analysis carried out in this work. The characterization of the model, the assumptions made and the results obtained. A discussion of the results is also present, with individuation of the issues to overcome.

The forth chapter represents a technical overview of the possible solution to improve the comfort quality of a vehicle. Advantages disadvantages for each of them are presented. A final choice of a suspension strategy has been finally recommended.

Chapter 2

Background

In the first part of this chapter a short introduction of in-wheel electric motors is given pointing out the main advantages and disadvantages. The second part instead is dedicate to introduce the fundamentals of ride comfort with the description of the procedure usually adopted to analyse the vertical vibration behaviour of a vehicle (road surface characterization, ride modelling, human sensitivity and performance criteria).

2.1 In-wheel electric motors

The idea of electric motors fitted inside the hub/wheel is not recent. The *Lohner-Porsche* car appeared at the World Exhibition in Paris in 1900 (Fig. 2.1). Although the performance of the car were remarkable for the times, the low battery capacities of the day was a too big obstacle to the diffusion of the idea. At the same time diesel and petrol engines increased remarkably their characteristics overtaking the transmission losses problems and becoming the standard as power supply for cars.

Nowadays with the growth of hybrid and electric cars scenario, in-wheel drive systems represent a valid alternative to central electric units. The most attractive reason in favour of this choice is with no doubts the possibility to eliminate completely the transmission.
Here the main *advantages* are sketched out:

- **Layout design.** Housing the drive system in the wheels gives greater freedom in designing the layout. and makes it easier to provide room for space-consuming components such as fuel cell stacks and hydrogen tanks.

- **Energy efficiency.** Without a transmission the energy lost in each gear or

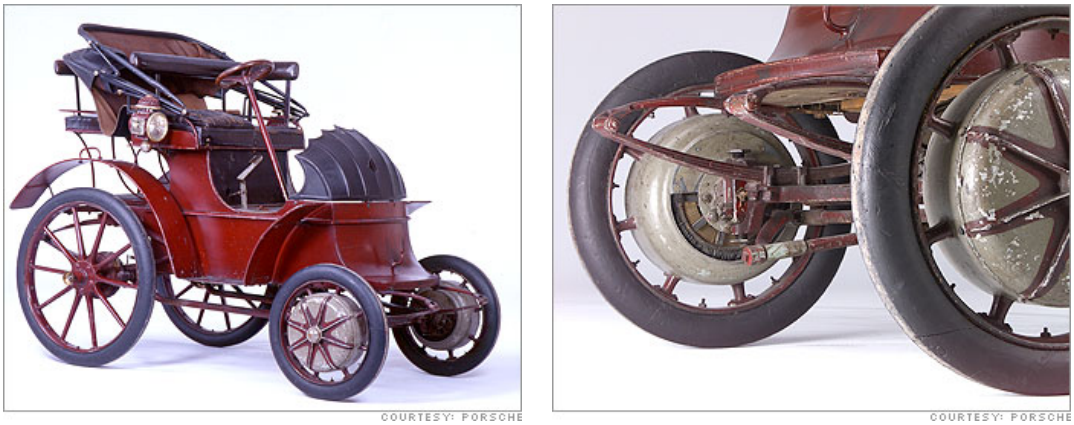

Figure 2.1 – First example of hub motor mount: *Lohner-Porsche* (1900).

joint otherwise is saved. For example is the efficiency of a Cardan joint is approximately $\eta_C = 0.99$ while is $\eta_d = 0.95$ for a standard differential.

- **Weight saving.** Although four small electric motors are surely heavier than a single motor having the same total power, it is true that this difference is largely compensate by the absence of all the transmission elements: gearboxes, differentials, drive shafts and axles.

- **Cost saving.** The manufacturing cost of all the transmission elements is widely higher than the cost of four electric motors.

- **Drive by wire.** Each wheel motors can be precisely electronically controlled and therefore, modern control systems such as ABS, traction control and stability control can become software functions and can be included at very little extra cost. Besides individual wheel control becomes possible enabling capabilities such as skid or four-wheel steering if desired.

- **Regenerative braking.** A three phase AC motor will easily turn into a generator any time the rotor is traveling faster than the applied drive frequency, which in practice is any time a vehicle is not accelerating. Naturally this improves also the energy efficiency.

- **Increased suspension options.** Without the conventional drive-shafts required to connect the wheels to the driveline is possible to implement a number of different suspension options otherwise difficult to develop.

On the other side in-wheel motors present *disadvantages* and difficulties to overcome:

- **Unsprung weight increasing.** As said before the unsprung mass increases considerably depending on the power of the motor. Furthermore the effect on the increasing of unsprung-to-sprung μ is more than proportional as it is joined with the reduction of the sprung mass caused by the absence of motors and transmission. This has implication (as it will be showed) for the ride of the vehicle.

- **Control.** Because of the absence of a mechanical differential it becomes necessary to replace by software and implement an individual wheel control in order to have acceptable level of skid.

- **Vibration effects.** The long-term durability effect of the high levels of vibration seen at the wheel is an area that will require careful engineering.

- **Wiring and cooling connections.** The connections required to the motor include wiring and possibly cooling. Depending on the level of electrical power demand and heat generated these connections can be not insignificant.

- **Isolation.** An electric motor placed inside the wheel is naturally more exposed to the action of water, mud, stones, etc., requiring then more attention on the design of protection systems.

A comprehensive description of all the in-wheel systems already available is out of the aims of this thesis. Nevertheless in Fig. 2.2 the Volvo and Mitsubishi mounts are showed as examples of practical realizations of the system described.

(a) Volvo mount (b) Mitsubishi mount

Figure 2.2 – Examples of in-wheel electric drives.

In Fig. 2.3 instead a possible solution for the suspension geometry is showed. It refers to the front suspension of the hybrid version of the Mitsubishi Lancer-Evo MIEV mounting a classic McPherson strut. Although this solution is relative to a medium car with technical specifications completely different from the *Hyrban* car ones, the picture points out how an in-wheel motor can be implemented in a classic suspension design with small difficulties.

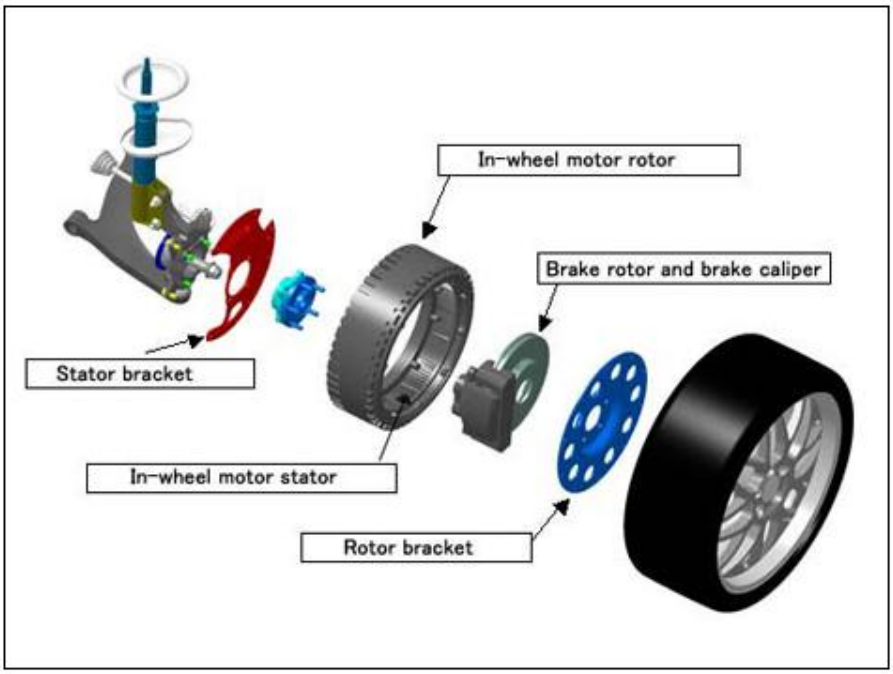

Figure 2.3 – McPherson strut with in-wheel electric motor.

2.2 Vehicle dynamics

Vehicle dynamics importance in design process of a new car has rapidly increased especially during last 15 years. The two main fields of study are the vertical and lateral dynamics (*Ride* and *Handling*), yielding to the definition and design of the principal vehicle subsystems. Besides, in order to a complete suspension design they need to be carried out also studies and simulations on longitudinal dynamics for the characterization of acceleration and braking manoeuvres.

As said in the introduction the area of interest of the present research is the ride, leaving handling studies to necessary further investigations in future. It seems useful at this point to present a justification why it is possible and acceptable to split in two aspects the same global phenomenon that is the vehicle dynamics.

2.2.1 Ride and Handling compromise

A commonly accepted approach has always been to study and develop ride and handling separately. This choice can be explained with a combination of theoretical and practical reasons ([2],[3]):

- The vehicle modes which dominate ride (bounce, pitch, roll, wheel vertical motions) are weakly coupled in a dynamics sense with those which dominate handling (lateral, yaw, forward speed, roll). In practical terms, this theoretical idea suggests that the forcing inputs in the vertical direction dominate motions in that direction (ride) and have little influence on lateral or yaw motions. Equally, lateral forces generated at the tyres completely dominate the handling response and have little effect on ride vibration.

- Secondly, the pragmatic reason is that it is preferable to reduce the scale of the analysis to manageable proportions.

Of course, this decoupling argument is not perfectly true as it is clear that the two aspects interact strongly with each other during practical driving; cornering manoeuvres occur on roads which provide vertical input disturbances to the suspension. Body roll, for example, can result from either uneven roads or cornering forces. Treatments of ride and handling together are rare in literature although developments in powerful computing techniques have leaded to interest in combined analysis. Anyhow if the studies are concerned with gaining some understanding and insight into vehicle dynamic response in order ultimately to influence practical design features, then it is justifiable to deal with ride and handling separately.

Another aspect that needs to be exploited is that the suspension design requirements which ride and handling are based on are fundamentally antithetical. In fact a suspension design addressed to privilege the comfort requirement, filtering the road uneveness, is naturally "softer" than a suspension born to meet the handling requests. The last will result "harder" with a rigid setting in order to be more direct and with a quicker reaction to the driver's input. For common passive suspension, this contrast has always been resolved by an opportune "compromise" between the two requirements, shifting the set towards "rigid" or "soft" according to the typology of vehicle. The new suspension systems as active, semi-active, or in general *controlled suspensions*, permit to avoid the compromise design. They can continuously adapt their characteristics according to road input, driver's demand, or other parameters, reaching a greater level of optimization in every situation of exercise.

2.3 Ride Comfort

The vibro-acoustic comfort of a vehicle represents one of the most important "perceived vehicle qualities" thus related with the subjective perception of the customer. For example other vehicle characteristics connected in some way with the human subjective aspect are style, ergonomics, thermal comfort, active and passive safety, performance, fuel consumption, etc.

The vibro-acoustic behaviour of a car is usually referred to as *N.V.H.*, acronym of *Noise, Vibration, Harshness*. The term *Ride-Comfort* is commonly used to refer only to vehicle vibrations perceived as mechanical disturb that is for frequencies approximately up to 20 Hz. For frequencies between 20 Hz and 100 Hz the vibrations are perceived both as mechanical and noise, while we only perceive noise between 100 Hz and 22 KHz (higher audible frequency by human ear).

A convenient Ride-Comfort analysis usually complies with the procedure showed by the scheme in Fig. 2.4. Clearly it is not compulsory but it helps for the comprehension of the mechanisms ruling the vibrational comfort in a passenger vehicle.

The procedure can be explained in three subsequent steps of analysis:

1. Individuation of the excitation sources representing the causes of vibrations. Usually they are subdivided in:

   - *External:* road profile (see § 2.3.1), aerodynamics, etc.
   - *Internal:* engine, transmission system, wheel imbalance, steering system, brakes, exhaust gases system, tyre non-uniformities, etc.

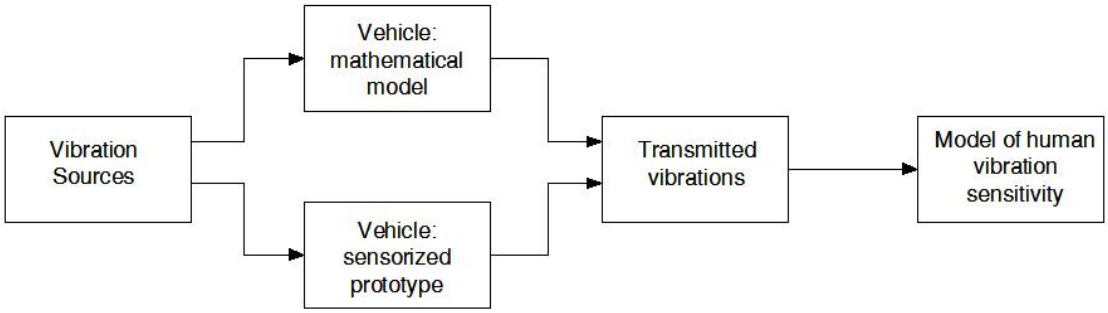

Figure 2.4 – Procedure adopted for Ride-Comfort analysis

2. Analysis of the vehicle vibration dynamics. The vibrations are transmitted at the the vehicle amplified or reduced. This analysis can be effectuated in two ways depending on the progress of the design process:

- *Mathematical modelling.* An analytical model of the vehicle is built in order to make an analytical study of the vibrations transmissibility. This methodology is helpful to predict the comfort levels of a car still under development.
- *Experimental test.* On a real vehicle the level of vibrations transmitted are measured with appropriate acceleration transducers usually placed in the vehicle/driver (or passengers) interface zones (steering wheel, seat, backrest and footrest).

3. The last step is the analysis of the effects of the calculated (or measured) vibrations on the human body. Although this part depends on subjective parameters, some standards (ISO 2631 and BS 6841) have proposed models and methodologies for the characterization of the human sensitivity to mechanical vibrations. Once obtained the vibration levels at which the passengers are exposed, these need to be weighted according to the human sensitivity models adopted (see § 2.3.3).

The absence of a traditional transmission system, exhaust system and internal combustion engine in the *Hyrban* car reduces the internal sources of vibration and constitutes a big advantage. To study the effects of the internal vibration sources on the vehicle and finally on the passengers is necessary to have precise information about all the design characteristic of the prototype. Being the component design still a "work in progress" it would be impossible to try to analyse their effect. Anyhow an internal source of vibrations that will need sure attention are the non-uniformities

of the tyre-wheel assembly. For standard wheels and tyres, shape, mass and stiffness irregularities may be cause of *static* and *dynamic* imbalances, source of vibrations transmitted to the whole vehicle [6]. The use of in-wheel electric motors amplifies these problems because of the peculiarity of the assembly. The bigger mass, the specifications of the electric motor, the presence of regenerative brakes, etc., are all factors increasing the difficulty of a correct wheel balancing. As said the present study does not take into account the effects of the internal vibrations source but further studies are strongly recommended during the next steps of suspension design.

Regarding to external vibration sources the aerodynamics has a minimal role in the ride-comfort behaviour of the *Hyrban* car. The prototype in fact is fundamentally a urban city car with a maximum velocity approximately of 80 Km/h (about 50 mph). Beside this peak velocity would be reached only in few occasion with an average life cycle velocity definitely lower. The aerodynamic effects are proportional to the square of velocity, therefore it has been chosen to neglect them.

The attention has been focussed only on the external vibrations coming from the road profile. Subsequently as suggested by the procedure described above, the basics on ride modelling and human response to vibrations are exposed. Finally common ride performance parameters are presented. They derive from the formalisation of desirable vehicle properties concerning vertical dynamics.

2.3.1 Road profile characterization

There are several road profile measurement techniques all addressed to obtain an accurate representation of the vibration input coming from the ground. However, none of the representations obtained can be said to match exactly with the real road profile. For this reason the road elevation profile is a classic example of *non-deterministic* function and then it is possible to refer to it as a *random signal*. In particular the road unevenness can be characterized by a random fluctuation of surface elevation about the nominal geometry of the profile. Despite that, common roads present some kind of statistical regularity, so that, at least for small lengths, the road elevation signal can be considered *stationary* and *ergodic* with evident advantages for their characterization.[1]

The frequency content of a road profile signal is usually described in terms of its PSD (*Power Spectral Density*) as a function of frequency either in radians or in cycles per unit distance. According to Wiener-Khintchine theorem the PSD of an ergodic random signal is defined as the Fourier transform of its *autocorrelation*

[1]Details on random signals theory can be found in [7].

function. Given for example an elevation profile $g(x) \in \mathbb{R}$, its spatial autocorrelation function $R_g(\tau_x)$ is defined as

$$R_g(\tau_x) = \lim_{L\to\infty} \frac{1}{L} \int_{-\frac{L}{2}}^{\frac{L}{2}} g(x)g(x+\tau_x)\,\mathrm{d}x, \tag{2.1}$$

where L represents the portion of road measured and τ_x is the incremental space between the values of g considered. The PSD of the profile is then the Fourier transform of $R_g(\tau_x)$

$$S_g(n) = \int_{-\infty}^{+\infty} R_g(\tau_x)\,\mathrm{e}^{-\mathrm{i}n\tau_x}\,\mathrm{d}\tau_x. \tag{2.2}$$

In this case the power spectral density unit is $\mathrm{m}^2/(\mathrm{cycles/m})$, if the profile g is expressed in meters and the spatial frequency (or wavenumber) n in cycles/m. The wavenumber is the reciprocal value of the wavelength λ (m).

Extensive measurements have shown that exists a typical pattern for the power spectral density of almost the totality of asphalted roads. It can be described by the following empirical formula:

$$S_g(n) = Bn^{-p}. \tag{2.3}$$

The term B represents a roughness coefficient which will be larger for rougher surfaces and smaller for smoother surfaces. In literature the term *unevenness index* can be found referred to the coefficient B. It is important to notice that $B = S_g(1)$. The index p instead, often called *waviness*, is the slope of straight line resulting from a log-log plot of the PSD curve espressed in (2.3). The unit of measurement of the coefficient B depends also on the value of the index p.

In Fig. 2.5 it is showed the power spectral density of a typical road. As expected long waves (hills and valleys) have large amplitudes while short wavelengths (microroughness) have small amplitudes.

Sometimes (as showed in Fig. 2.5) the equation is given with a discontinuity in slope and two values of p are necessary to represent the dual slope:

$$S_g(n) = \begin{cases} B\left(\dfrac{n}{n_0}\right)^{-p_1} & \text{if} \quad n \le n_0 \\ B\left(\dfrac{n}{n_0}\right)^{-p_2} & \text{if} \quad n > n_0 \end{cases} \tag{2.4}$$

where n_0 is the wavenumber of the discontinuity. An equation of this form implies

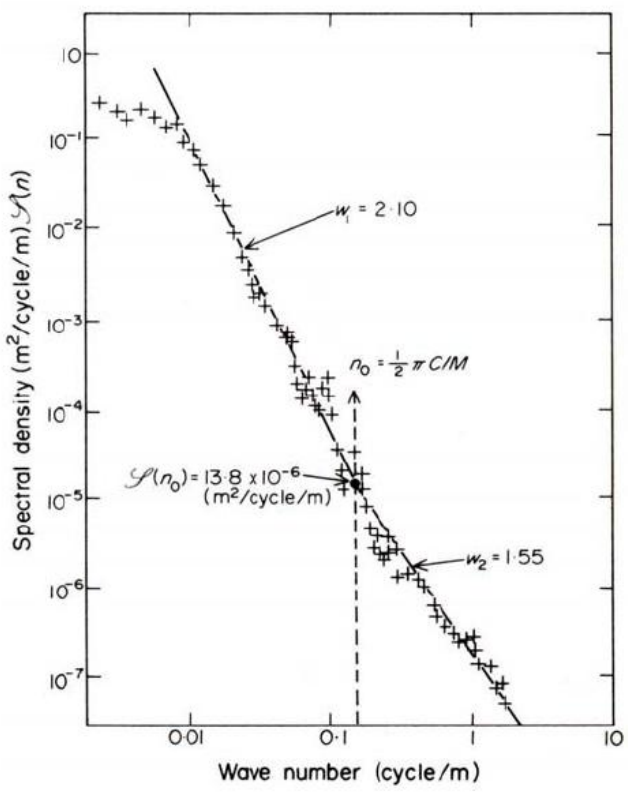

Figure 2.5 – Power spectral density of a typical principal road

that for low wavenumber the amplitude tends to infinity. Naturally this is not true and it can be taken into account introducing a cut-off wavenumber n_{co} below which the amplitude spectral density remains constant. Anyhow for general purpose modelling it is sufficient to assume the input spectrum has a single slope. In Tab. 2.1 the values of roughness coefficient B and index p are indicated for typical surface roads with *range* and *mean* values [10].

Surface	B (range)	B (mean)	p (range)	p (mean)
Motorway	$3 \cdot 10^{-8}$ — $5 \cdot 10^{-7}$	$1 \cdot 10^{-7}$	2 — 4	2.5
Principal Road	$3 \cdot 10^{-8}$ — $8 \cdot 10^{-6}$	$5 \cdot 10^{-7}$	2 — 4	2.5
Minor Road	$5 \cdot 10^{-7}$ — $3 \cdot 10^{-5}$	$5 \cdot 10^{-6}$	2 — 4	2.5

Table 2.1 – Surface roughness coefficients for typical roads

As far as this point only the objective roughness properties of the road surface have been considered. In order to study the road profile as a temporary input for

mathematical vehicle models it is necessary to consider the velocity which the profile is traversed with. If a constant value of velocity v is assumed, the profile $g(x)$ may be expressed with a temporary law $h(t)$ with $h(t) = g(vt)$. Considering the relation between spatial and temporary frequency

$$f = nv, \tag{2.5}$$

it is possible to correlate $S_h(f)$, spectral density of the temporary signal $h(t)$, with $S_g(n)$, spectral density of the road profile $g(x)$, then with a PSD in terms of frequency rather than wavenumber:

$$S_h(f) = \frac{S_g(f/v)}{v},$$

where $S_h(f)$ is expressed in m^2/Hz, and the frequency f in cycles/s.
According to (2.3) it derives that

$$S_h(f) = \frac{Bv^{(p-1)}}{f^p}. \tag{2.6}$$

The previous equation clearly shows how increasing the velocity v has the same effect on the input to the suspension as having a road surface deterioration.[2] In fact the characterization of the road profile, given by (2.6) in terms of PSD vs frequency, clearly depends on the value of the travelling velocity v. In Fig. 2.6 it is showed, for a given velocity $\bar{v}$, the PSD of a given road profile elevation in terms of frequency. In the same figure are also represented the pattern of the velocity and acceleration of the road profile covered with velocity $\bar{v}$. It is clear how the contribution at the PSD for the acceleration becomes relevant at high frequencies.

2.3.2 Ride modelling

The next step of the procedure indicated at pag. 15 is relative to vehicle ride modelling. According to the level of accuracy we need to reach, different models can be adopted with respective assumptions and simplifications. Naturally a vehicle, being a continuous body, has infinite modes of vibration each one with its characteristic natural frequency. The most accurate a model is, the more degrees of freedom includes.

A conventional subdivision of the frequency spectrum of the vibrations for common passengers cars, has been proposed by SAE organization (*Society of Automotive*

[2]This effect can be easily understood thinking that everybody tends to slow down while driving from a surface road to a rougher one.

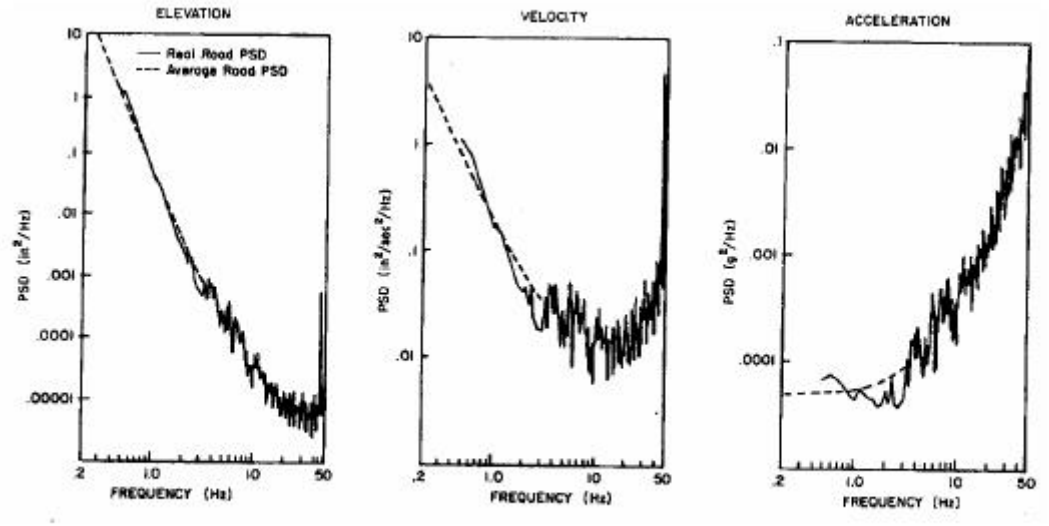

Figure 2.6 – PSD's of elevation, velocity and acceleration of a road profile

Engineers), and is schematically showed in Fig. 2.7. Formally five main perception frequency ranges have been individuated, although it is clear how it has no sense to think to exact frequency limits but it would be more convenient to define also transition zones.

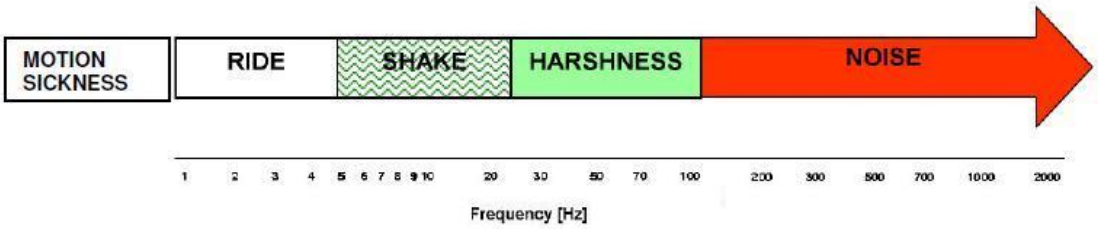

Figure 2.7 – Conventional subdivision of the frequency spectrum.

The five frequency ranges are:

- **Motion sickness:** vibrations with frequency lower than 0.5 Hz. They are associated with the natural frequency of the internal human organs. Almost the totality of the vehicles can be considered as a static system as the excitation frequency is lower than their first natural frequency.
- **Ride:** low frequency vibrations of the car body (up to 5 Hz). All the vehicle subsystems can be considered to behave like rigid bodies. It is also called *Primary Ride*.

- **Shake:** medium frequency vibrations (5–25 Hz) sometimes involving the first bending modes of the vehicle chassis (often named *Secondary Ride*).
- **Harshness:** higher frequency vibrations (25–100 Hz) of the vehicle structure and/or components, partly perceived as noise. If these vibro-acoustic phenomena are particularly strong (being amplified by vehicle acoustic cavity), the term *Boom* is often used.
- **Noise:** vibro-acoustic phenomena with frequency range beyond 100 Hz.

It is important to underline how the previous subdivision was developed for normal production cars. Thus for other vehicles it may not be useful. Every single vehicle in fact has its own natural frequencies that may vary considerably from the reference ones, especially in case of particular vehicles (e.g. race cars, micro-cars, buses, etc.). Nevertheless a standard subdivision is useful to a logical approach of suspension sub-systems design. The design of the so called primary elastic elements, such as springs and roll-bars, is strictly connected to the primary ride frequency range. The secondary ride frequency instead is relative to design and characterization of the secondary suspension elements such as bushings and shock absorber pads.

Typical examples of resonant frequencies for the main subsystems of a reference vehicle are:

Body resonance	1–1.5 Hz
Wheel hop	10–12 Hz
Passenger on seat	4–6 Hz
Engine/gearbox on mounts	10–20 Hz
Structural resonances	> 20 Hz
Tyres	30–50 Hz (first mode)
	80–100 Hz (second mode)

Considering the *Ride* and *Shake* frequency range, they roughly correspond to the passage on undulations of the road. In this band of frequency the modes of vibration of the vehicle are characterized by the rigid motion of the front and rear frames, by the travel of the suspensions and by the deformation of the tyres.

The ride and shake range is the most important from the point of view of comfort for the following reasons:

- the human sensitivities to whole-body vibrations and to arm-hand vibrations (as it will showed in the next section) peak respectively in the ranges 1–8 Hz and 12–16 Hz;

- in this range the spectrum of vibrations generated by road unevenness (§ 2.3.1) still shows relevant amplitudes.

The attention is then focussed on the design primary suspension elements according to ride-comfort needs in the ride and shake bands of frequency.

Classic ride models

The mathematical models that can depict the characteristics of a vehicle in the range of frequency exposed are very simplified having few degrees of freedom and adopting strong assumptions. The common models used in literature are the so called "Seven Post" with seven degrees of freedom (7dof), the "Bicycle model" with four degrees of freedom (4dof), and the most used "quarter car" model with only 2 degrees of freedom (2dof), also known as *De Carbon* model. Despite the reduced number of degrees of freedom adopted these models represent the standard for a primary ride analysis and permit to catch almost all the main suspension characteristics.

The assumptions and simplifying hypotheses made for all of them are briefly summarized:

- The mass of the vehicle is subdivided into a *sprung mass* m_s, and one or more *unsprung masses* m_u. The first represents the body of the vehicle suspended on the springs (chassis, engine, passengers, etc., whereas the second are the remaining "not suspended" parts (wheel, hub, parts of the suspension elements, brakes, etc.). Both of them are considered as rigid bodies.

- The models are relative to the case of vehicles travelling at constant velocity on a straight road.

- The suspension behaviour is considered *linear*. Both the wheel rate k_s and the shock absorber coefficient c_s are constant. The elastic force is considered as a linear function of the wheel travel, while the damping force as a linear function of the wheel vertical velocity. This is probably the strongest assumption made by these kind of models. In fact both the elastic and the damping elements have non-linear characteristics. The assumption made on the elastic element anyway is more plausible: the elastic function is a function with continuity class C^1 then, considering small wheel travel differentials is always possible to linearize with a good according on results. The damping function instead has continuity class C^0, having a first derivative discontinuity in the origin. This

kind of non-linearity cannot be moved around needing numerical tools to be treated or advanced mathematical models for an analytical approach.

- The engine suspension is not modelled. The engine mass is then part of the rigid body mass m_s.
- Apart from the advance velocity, the axles are assumed to have only the vertical motion. Their pitch or longitudinal motions are generally very limited with natural frequencies much higher than the ride and shake range.
- As the wheels as almost a translatory motion, their rotation is considered as dynamically not influential so it is neglected from the models.
- The seats are not modelled. Surely they contribute to raise the level of comfort but their characterization is not straightforward so it is usually not considered. The models results then conservative in this sense.
- The tyre is modelled as a linear spring with coefficient k_t. The range of frequency considered permits to avoid an accurate characterization of the tyre as its natural frequencies are all in a higher range. A linear characteristic of the spring is considered a valid hypothesis only for small compression and moderate velocity of the car.
- The contact between tyre and road profile is considered as a point with the tyre following all the asperities. It can be showed that in reality the width of the tyre edge on the road surface is often smaller than the wavelength of the roughness (at least for small frequencies). This gives a justification of the model.

Next a short description of the peculiar assumptions made for each of the reference models is presented. The equation of motion are not reported as the aim of this section is just to present schematically the most common models used in literature.

Seven post model (7dof)

In Fig. 2.8 is showed the scheme of the *Seven post* model. The rigid body has mass m_s and pitch inertia J_θ and has freedom to move in pitch, roll and bounce. The vertical motion of the front wheels contribute a further two degrees of freedom, whilst the remaining degrees of freedom are either the independent vertical motion of the rear wheels, or the bounce and roll motion of a rear axle. Although the

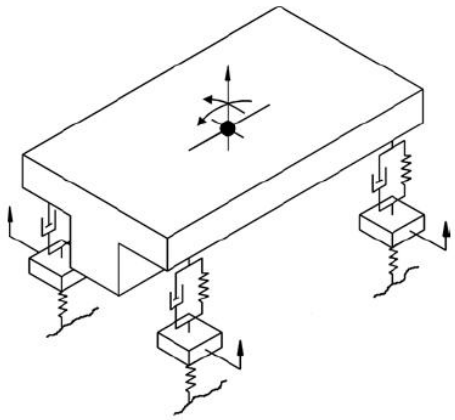

Figure 2.8 – Seven post model (7 dof)

apparent simplicity of the model, it is still hard to manage manually and requires numerical tools to be analysed. Besides, the information obtained are difficult to be worked out for a basic ride comfort analysis. Further reductions can be done.

Bicycle model (4dof)

The bicycle model in Fig. 2.9 results the closer reduction from the previous 7dof model. The further assumption made are all in the direction of creating a two-dimensional model (2-D). The road surface generally cannot be considered as cylindrical. Besides the input profile on the left side is not strictly correlated with the right side. Statistically talking it is possible to introduce a coherence function between left and right profile, where the smaller is the vehicle track and the bigger is the coherence. Despite that they can be done the following considerations:

1. For long wavelengths, the coherence between the left and right tracks is likely to be high, and the road surface may be regarded as cylindrical. Consequently the two sides of the vehicle will behave in a similar fashion.

2. For shorter wavelengths the motions excited in the vehicle will mostly involve wheel hop. Little body motion will occur, and right and left will interact very little.

3. All the vehicles can be considered as almost symmetric as regard of their longitudinal vertical middle plane.

The previous considerations can represent both a justification of model and the limits of validity of it. For example if it is necessary to study the behavior of a

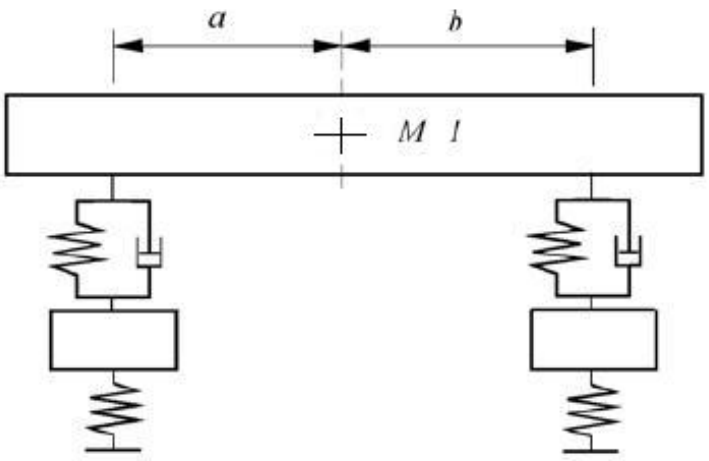

Figure 2.9 – Bicycle model (4 dof)

vehicle traversing a road with a small coherence between left and right track (e.g. an off-road path), the bicycle model becomes scarcely realistic.

Quarter car model (2dof)

A further reduction of the bicycle model is represented by the quarter car model that it the simplest way to represent the vertical behaviour of a suspended vehicle (Fig. 2.10).

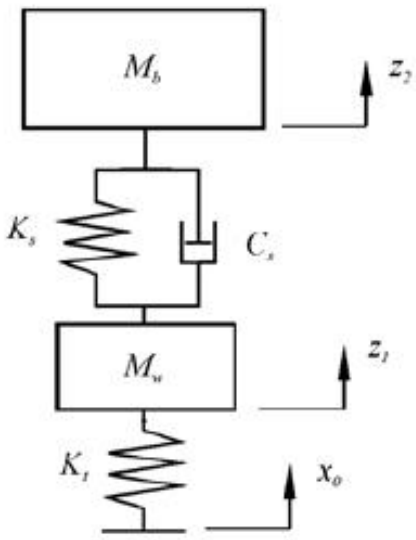

Figure 2.10 – Quarter car model (2dof)

The model may be intended in two different ways:

1. The first approach is to consider the model as representative of the whole vehicle. That means that the sprung mass M_b is the total mass of the body of the car, while the unsprung mass M_u is the sum of all the unsprung masses of the vehicle. The implicit hypothesis is then that the only motion depicted by the model is the vertical one. The unsprung masses are considered as rigidly linked and pitch motion is neglected. The elastic element coefficient k_s is then the sum of the front and rear wheel rate k_{s_f} and k_{s_r} that are considered in parallel configuration. The same happens for the damping wheel rate c_s sum of the front and rear damping coefficient c_{s_f} and c_{s_r}.

2. The second approach derives more directly from the bicycle model described above. Making assumption on the mass distribution on the vehicle it is possible to "isolate" the single suspension decoupling it from the other one. (This gives sense to the name *Quarter car* or *Mono-suspension* that the model has.)

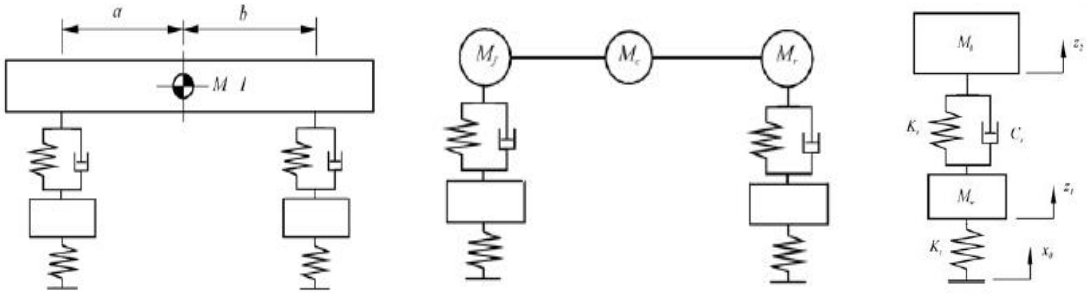

Figure 2.11 – Justification of the quarter car model

The steps bringing from the 4dof to the 2dof according to the second interpretation (or justification), are next described and showed in Fig. 2.11. The first step is to replace the bicycle model to a "dynamically equivalent" system (Fig. 2.11(b)). The three mass system is equivalent to the rigid beam system if the following conditions are true:

- the total masses are equal

$$M_f + M_c + M_r = M, \tag{2.7}$$

- the masses centres are in the same position

$$M_f a = M_r b, \tag{2.8}$$

- the pitch inertias are equal

$$M_f a^2 + M_r b^2 = I. \tag{2.9}$$

It can be shown that $M_c = 0$ if $I = Mab$. This condition is very close to practical realizations as we have that $I \approx Mab$ for almost all the commercial vehicles. The previous condition implies that there is no interaction, or at least very small, between front and rear axles. This permits to "isolate" the single suspensions, studying separately two sub-problems, the front suspension determining the the motions of M_f, the rear suspension those of M_r, while the motions of the points within the wheelbase are determinable by geometric proportioning (Fig. 2.11(c)). So each sub-problem requires only a quarter vehicle model for its examinations (Fig. 2.10).

2.3.3 Human sensitivity to vibrations

Once the dynamic analysis of a vehicle has been conducted (through numerical simulations of a mathematical models, or through experimental test) the data obtained define the levels of vibration the driver (and passenger) is exposed to. These vibrations are transmitted through the driver-vehicle interfaces (steering wheel, seat, back, footrest) as showed in Fig. 2.12. It has been studied that the vibration com-

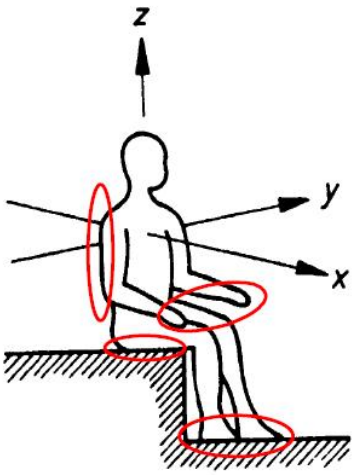

Figure 2.12 – Driver-vehicle interface areas

fort is strongly connected with the acceleration levels. It is convenient to consider an average acceleration value. It is common to adopt the *Root Mean Square* value (RMS) of the acceleration at the generic interface defined as follow:

$$\text{RMS } a(t) \equiv \tilde{a} \equiv \sqrt{\frac{1}{T}\int_0^T a^2(t)\,\mathrm{d}t}, \tag{2.10}$$

where $a(t)$ is the acceleration signal measured for a time interval T. But in order to define a comfort index, it cannot be used the acceleration signal as measured. In fact several experiments, conducted at the beginning of the last century on sample groups of people to study the comfort of public transportation buses, have showed that human reaction to vibrations is a phenomenon strongly non-linear depending on the characteristics of the vibration signal:

- Magnitude and frequency;
- Input position and direction;
- Duration of excitation.

Despite that, response and human reaction to vibration is fundamentally a subjective matter, also influenced by external factors (expectation, motivation, fatigue, arousal, personal variations, etc.). For this reason the subject is still a specialist area of studies. The most up to date reference to treat this matter is the international standard ISO 2631-1 (1997), which describes a methodology to quantify the effects of mechanical vibrations on whole human body. The original studies described above are the basis of the ISO 2631 standard. They defined curves of sensitivity at the variation of the vibration characteristics listed above.
Three acceleration limit levels were specified:

1. exposure limit, implying damage to health;
2. fatigue decreased proficiency, implying an impaired ability to perform tasks;
3. reduced comfort.

In Fig. 2.13, for example, the curves relative to the 2° criterion are showed. Practically they represent curves of iso-working efficiency at the variation of amplitude, frequency and exposure duration of the vibration input. The left graph is relative to vertical vibration (z direction), whereas the right one to the horizontal vibrations (x and y directions). The acceleration amplitude limits are expressed in terms of RMS

against frequency. The range of frequency considered is 1–80 Hz. The minimum acceleration areas correspond to the frequency range where the sensitivity is greater. In fact the levels of acceleration amplitude relative to a decreased working efficiency are smaller on equal terms of time of exposure. The maximum sensitivity range are then 4–8 Hz for vertical vibrations (linked with the natural frequencies of the internal human organs), and of 1–2 Hz for lateral vibration (linked with the chest and head motions).

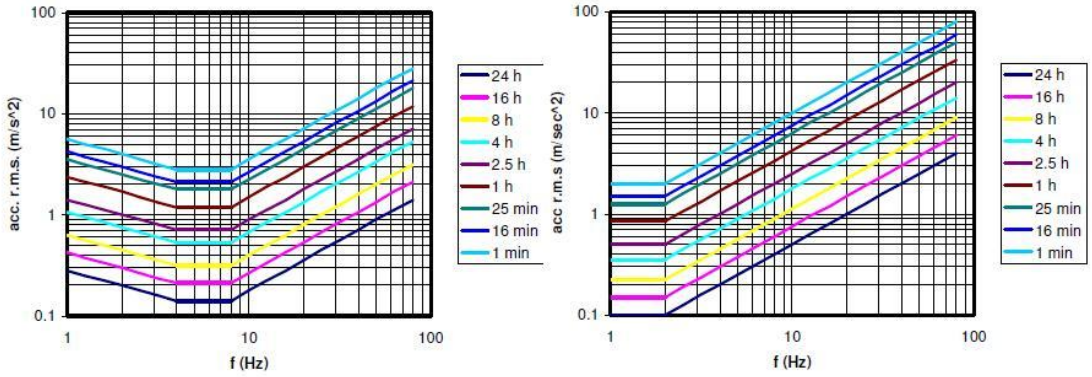

Figure 2.13 – Sensitivity curves relative to the "fatigue decreased proficiency" as given in standard ISO 2631. (Left: z-axis vibration; Right: x- and y-axis vibration)

In order to consider the different sensitivity showed by the graphs above, the ISO standard suggests the adoption of *frequency weighting filters* for all the range 1–80 Hz. In this way all the acceleration values, in the frequency range considered, have the same weight in terms of human sensitivity. In Fig. 2.14 it is showed the weighting filter relative to z-axis. The filter is applied to the vertical acceleration measured (or calculated) coming from the seat (or from the footrest). The correlation with the sensitivity graphs showed in Fig. 2.13 it is clear noting that within the range 4-8 Hz, area of maximum sensitivity, the magnitude is zero, whereas for all other frequency the signal is attenuated.

An example of the effect of the weighting functions on a signal is showed in Fig. 2.15 where the filter function W_k has been applied to the experimental z-axis acceleration signal recorded at the seat of a motorcycle passing on a cobblestone track at the velocity of 30 km/h. The peaks amplitude of the signal are lightly reduced and the high frequency components have been "cut" by the filter.

They have been yielded weighting functions for all the direction of vibration. Thus the generic input acceleration signal $a_{ik}(t)$, representing the component in direction i of the acceleration measured at the generic driver-vehicle interface k,

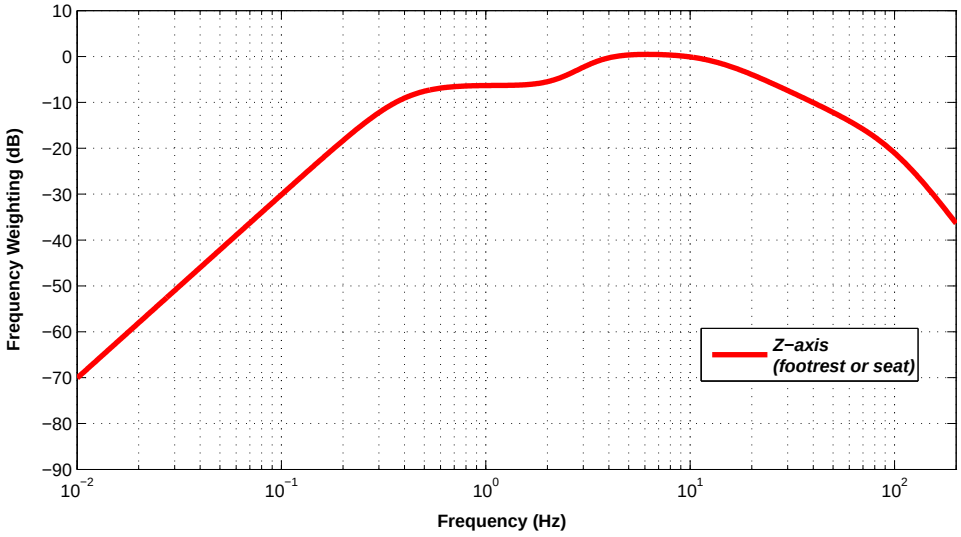

Figure 2.14 – Frequency weighting filter W_k for vertical accelerations

may be "weighted" with the corresponding filter, becoming a new signal $a_{ik,\mathrm{w}}(t)$. In succession the RMS value is calculated:

$$\tilde{a}_{ik,\mathrm{w}} = \sqrt{\frac{1}{T}\int_0^T a_{ik,\mathrm{w}}^2(t)\,\mathrm{d}t}. \tag{2.11}$$

In succession is possible to obtain an equivalent weighted RMS acceleration for the generic interface point k summing the components in the three directions weighted again with coefficients k_i given by the ISO standard:

$$\tilde{a}_{k,\mathrm{w}} = \sqrt{(k_{xk}\tilde{a}_{xk,\mathrm{w}})^2 + (k_{yk}\tilde{a}_{yk,\mathrm{w}})^2 + (k_{zk}\tilde{a}_{zk,\mathrm{w}})^2} \tag{2.12}$$

Finally it is possible to define a whole comfort index including all the driver-vehicle interfaces k and representing an equivalent acceleration RMS value. At this purpose the standard ISO 2631 introduces the index VTV (*Vibration Total Value*) defined as follow:

$$\mathrm{VTV} \equiv \sqrt{\tilde{a}_{\mathrm{footrest,w}}^2 + \tilde{a}_{\mathrm{seat,w}}^2 + \ldots}, \tag{2.13}$$

where all the possible interface measured signals are summed by means of their RMS weighted value.

If the acceleration signal has significant peaks, it is defined a different index created to consider the bigger discomfort deriving from accelerations varying of big entities in a short time period. The calculation depends on the *crest factor*, which is defined as the peak value divided by the RMS value of the acceleration. If the

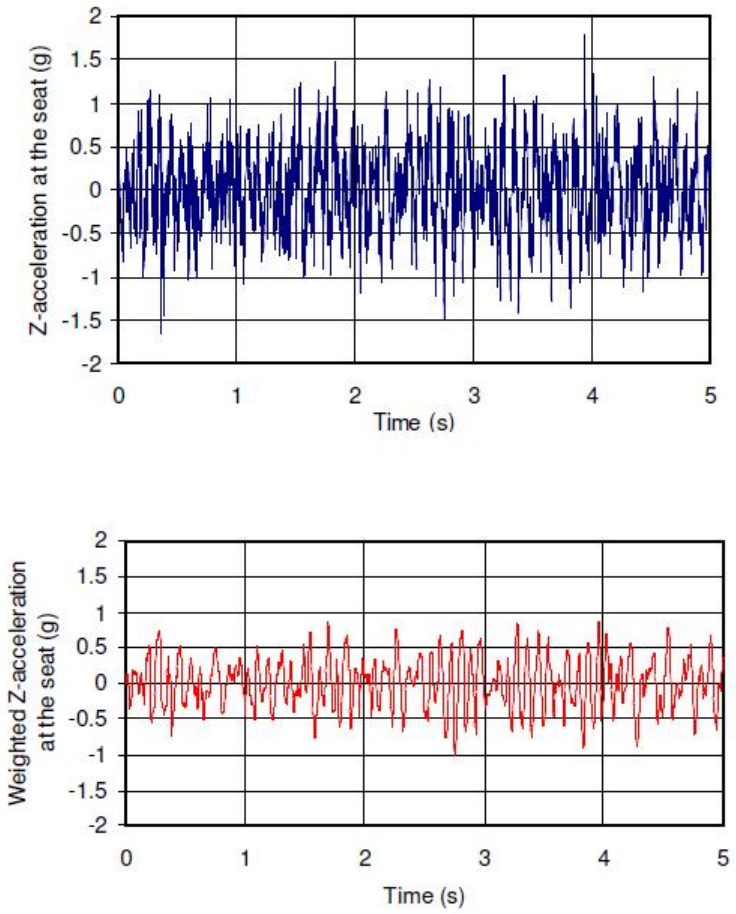

Figure 2.15 – Effect of the weighting function W_k

crest factor after weighting exceed 6, then a VDV (*Vibration Dose Value*) index is defined:

$$\mathrm{VDV} \equiv \sqrt[4]{\int_0^T \tilde{a}_{\mathrm{w}}^4(t)\,\mathrm{d}t} \tag{2.14}$$

The VDV has not the same meaning of the VTV having different units of measure.

The effects of rotational accelerations and vibration coming from other interfaces (steering wheel, gearshift) can be computed in analogous way following the procedure described by the ISO standard.

Contrarily to the dated version of the ISO standard (1985), the current standard does not contain vibration exposure limits, because many factors combine to determine the degree to which discomfort possibly will be noted or tolerated. In addition, interference with activities (e.g. reading, writing and drinking) due to vibration and many other factors (acoustic noise, temperature, etc.) could sometimes be considered as a cause of discomfort. For these reasons, only evaluation methods have been

defined in the standard, so that they can be utilized as the basis for limits which may be prepared separately. In any case, Vibration Total Value, VTV, defined in (2.13) might be compared with the guidelines values in Tab. 2.2, giving approximate indications of likely reactions to various magnitudes of overall vibration total values.

VTV range (m/s^2)			Comfort level
0	—	0.315	not uncomfortable
0.315	—	0.63	a little uncomfortable
0.5	—	1	fairly uncomfortable
0.8	—	1.6	uncomfortable
1.25	—	2.5	very uncomfortable
2	—	$+\infty$	extremely uncomfortable

Table 2.2 – Guideline of comfort levels related to VTV threshold values

2.4 Suspension performance criteria

Taking into account only the ride behaviour, the specification of the desired properties of a passenger car is quite straightforward. Beside the comfort requirements already discussed, other primary suspension issues, related with traditional passive systems, are individuated: the suspension working space, the wheel load variation, the static and dynamic attitude control, the contribution to good steering behaviour. Considering also controlled suspension systems, important aspects are also the power consumption and the actuator forces. With a mathematical modelling approach, the number of information available on the suspension characteristics are proportional to the complexity level of the model. The quarter car model permits to characterize the main suspension issues with small amount of parameters.

In Fig. 2.16 the performance parameters usually adopted are showed with their characterization in a simple quarter car model. Naturally the pitch and roll body attitude cannot be derived from a 2dof model, needing at least a 4dof model (bicycle model) for pitch or a 7dof to include also the roll.

Next the three main parameter usually taken into account are described:

Discomfort parameter (ACC). This parameter is equivalent to the VTV comfort index described in the previous section. It consist in the RMS value of the vertical frequency weighted acceleration. The ACC is then referred to

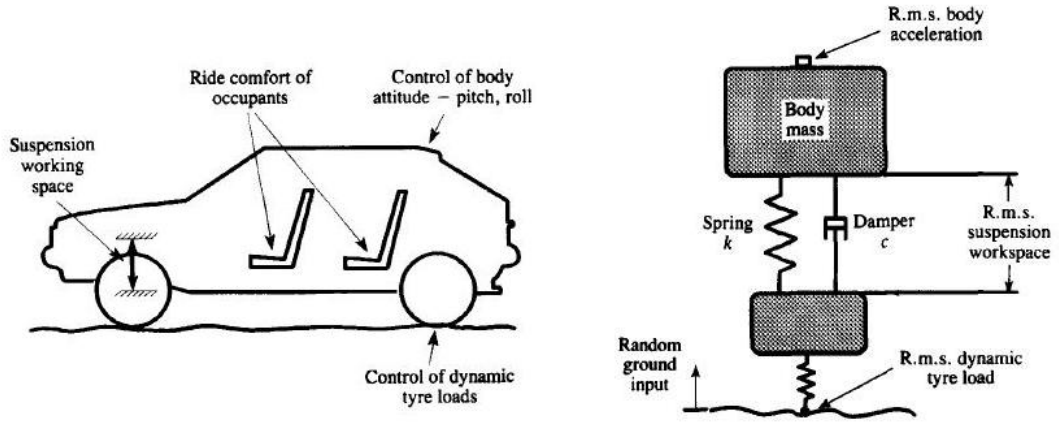

Figure 2.16 – Ride performance criteria and quarter car model characterization

quarter car models where the only body acceleration recorded is the vertical acceleration in the z-axis. Vertical acceleration, in fact, is likely to dictate the ride quality in any case, being lateral and rotational motions considered as secondary aspects.

Suspension working space (SWS). Defined as the RMS value of wheel to body displacement, this parameter measures the variation of the displacement about its static position. The importance of this parameter is due to several reasons. The most important are:

- Packaging and layout constrains. The availability of space is usually very limited being a constrain for the maximun suspension working travel.
- Lateral vibrations. The more the working travel, the more the lateral flexibility, with incoming problems related to lateral vibrations. Therefore in a suspension like the McPherson strut, an high suspension working travel could rise problems of "damper hysteresis" due to the bigger moment the damper stem would transmit to the gasket with consequent bigger friction and possible oil-seal problems. This would also increase the superficial wear of the damper stem snd deteriorate the comfort because of *stick and slip* phenomena.
- Body motion. Even if the model adopted is a 2 dof, a great SWS means bigger pitch and roll angles before that the suspension come to bump end stop rubber. In fact it is necessary that the suspension end stops come into contact only during extreme occasion (as pothole, off-road, etc.),

then the suspension displacement has to remain inside predefined limits. It must be said that in reality the geometry of the suspension, and then the wheel rate, have a fundamental role on the control of body motions. The considerations made then lose their validity in case of wheel rate values far for standard ones.

Dynamic tyre load (DTL). Defined as the RMS value of tyre load variation about the static value, this parameter can be considered a measure of road holding ability, since a variation in the tyre load results in a varying contact length and a net reduction in side or braking force. When a lateral or longitudinal force is demanded from a tyre, the contact patch must distort before the force can be fully generated. This distortion requires that the tyre rolls round a certain distance and hence there is a small time delay before the full force is available. Under dynamic conditions when the tyre load is fluctuating due to suspension movements, the effect of this dynamic lag mechanism in the tyre is that the effective lateral and longitudinal forces available are reduced. Overall, the maximum forces are available if the vertical tyre load on the tyre is steady and they reduce as the dynamic fluctuations increase.

2.5 Suspension strategies

The aim of this section is to give a very short overview of the "strategies" that it is possible to adopt in a all kind of suspension designs. The following subdivision then is independent from the different geometries a suspension can have. Up to present the technically available strategies that is possible to adopt are next described:

Passive systems. Passive systems are considered to contain conventional springs and shock absorbers (dampers). These systems contain no sensors, electronics or controls. The only possible addition of a self-levelling system which typically involves time delays of many seconds and which is designed to compensate for variations in static load. Passive suspensions are the most common type of system used for their simplicity. The main disadvantage is that is not possible to optimize all the performance criteria with this kind of suspension, usually needing a trade-off between comfort and road holding.

Active systems. Active suspension system are thought of as, at least in part, replacing the springs and shock absorbers of passive system by actuators which act as force producers according to some control law. The actuators operate with force transducers providing inner loop feedback signals to their controllers and are imagined to track faithfully a force demand signal determined by the control law. the control law may contain information of any kind obtained from anywhere in the system, and an important part of the active system design problem is the determination of the control law which will give a good system performance. It is implied in the description that the actuator control bandwidth extends to substantially beyond the wheel hop frequency, determined by the unsprung mass and tyre stiffness and typically near to 10 Hz.

Semi-active systems. Semi-active systems derive from, and closely related to the active systems just described. The difference is that the actuators are replaced by *controllable dampers*. These too are thought of as employing force inner loop feedback control to track a force demand signal which is a replica of the corresponding active system, except that in circumstances where the active system would supply work, the force demanded of the damper is zero. A semi-active system for an automobile requires a spring to support the body weight in parallel with the continuously variable damper. Unless otherwise indicated, the spring is thought of as having fixed characteristics.

Slow-active systems. Slow-active systems are thought of as active systems as de-

scribed before, except that the actuator control bandwidth is much reduced, embracing the normal range of body resonant frequencies in bounce, pitch and roll, and the frequency range of interest as far as responses to steering control are concerned, but not extending as far as wheel hop frequencies. Actuators can be either of two basic types:

1. *Flexible.* When they become inactive in a control sense (beyond the bandwidth), being flexible like a spring, they can support the body weight or act in *parallel* with the primary elastic element. Pneumatic actuators would be of this typology.
2. *Rigid.* They can be rigid when become inactive, in which case they must be mounted in *series* with the spring (or other elastic element). Spool valve controlled hydraulic actuators and electric motor/irreversible lead-screw actuators are example of rigid elements for slow-active suspensions. The intrinsically rigid type of actuator is better treated as a displacement producer rather than a force producer. Its inner control loop would involve displacement feedback and the actuator demand signal will notionally be a desired displacement.

Preview is what characterize active, semi-active and slow-active suspension from the passive ones. In fact it involves the acquisition and use for actuator control purposes of information relating to the profile ahead of the vehicle wheels. It will be taken to include the use of front axle derived information in order to improve the rear axle actuator control laws under the assumption the the displacement input to the rear wheels is a time delayed version of that to the front wheels.

In conclusion it the essential difference between passive and other systems is that the latter contain a measurement system and a control law such that some adaptive capability is virtually implicit in their design.

Chapter 3

Analysis

In this chapter is presented the frequency analysis of a simple "quarter car" with linear characteristics. The model has been put in state space form. The output vector has been created in a way to represent the comfort and suspension performance indices easily. They are underlined the effects of the *Hyban* lightweight and of the human sensitivity filter on the response functions of the system. After that simulations have been carried out in order to depict the variation of the suspension indices with the increase of the mass ratio μ.

3.1 Vehicle data

At the moment when this thesis work began, the technical specifications about the *Hyrban* project were very few. The only available data were roughly the dimensions, the overall weight, and the maximum power available. In fact as said before, this work is fundamentally a feasibility study with the main objective to find the weak point of the idea. The reference point about dimension can be found in a Smart car. Regarding instead power and weight, *Hyrban* and Smart cannot be compared with the first being much lighter and less powerful than the second one. The maximum velocity of the *Hyrban* car is about 80 km/h ($\approx$ 50 mph). In Tab. 3.1 the main data about the vehicle are reported. They represent the starting point of our analysis.

The curb weight of 350 kg indicated in the previous table represents a kind of limit or maximum weight. In fact one of the main characteristic of the project is the lightweight. This value is the maximum possible weight in order to achieve levels acceleration comparable with a Smart car. As the fuel-cell power is very small and even if there are the ultracapacitors recharged by the regenerative braking, it is clear

Wheelbase = 1.8 m	Track = 1.3 m
Curb weight = 350 kg	Fuel-cell power = 6 kW
Fully laden weight = 500 kg	Maximum speed = 80 km/h

Table 3.1 – Hyrban data

how the weight factor is very important. The fully laden weight of 500 kg includes the weight of the two passengers.[1] So in the sequent analysis the fully laden weight will be considered.

Analysing the effect of the increasing of the vehicle unsprung mass then, the previous considerations about the maximum possible weight become important. In all the traditional analysis in literature it is simply taken into account an increasing of the unsprung mass m_u with the consequent increase of the total mass M. For what said before instead, in this study the total mass is hold steady while the unsprung-to-sprung mass ratio μ increase. For this reason the masses conventional subdivision is made as follow:

$$\mu = \frac{m_u}{m_s}, \qquad m_s = \frac{M}{\mu + 1}, \qquad m_u = \frac{\mu M}{\mu + 1}, \tag{3.1}$$

where m_u and m_s become then function of the mass ratio μ, but also of the total mass M.

A further justification to this definitions can be found thinking that there is a kind of "mass transfer" between sprung and unsprung mass. In fact on a traditional hybrid vehicle the electric motor is mounted on the chassis and transmission joints are present. With this kind of new philosophy vehicle the mass the mass of the motor is transferred on the wheel and the mass of the joint can be thought as transferred on the regenerative braking system otherwise not present on the traditional car. In this way increasing the mass ratio μ is like increase the quantity of mass to be transferred from sprung to unsprung mass. The results of the analysis will then be an answer about how much it is possible (or recommendable) increase the mass ratio.

[1] According to the Dir. EU 95/48/EC, each passenger mass is considered to be equal to 75 kg.

3.2 Quarter car model

The first model to be analyzed is the classic "quarter car model" showed in Fig. 3.1. The total mass is divided into 2 rigid masses having only the vertical degree of freedom. Although its simplicity it permits to catch most of the ride characteristic of a vehicle with small amount of calculation a with good approximation. The model is supposed to travel with a velocity v on a road profile that represents the vibration input of the system. As said in the previous chapter the quarter car model can be interpreted in two different way. The first one considers the sprung mass as the total weight of the chassis and the unsprung mass as the remaining mass of the vehicle that is supposed to be rigid. In this way the vehicle only the vehicle bounce is depicted not taking into account the pitch. The second possibility is to consider the quarter car model as the front (or rear) suspension (see § 2.3.2). In this work has been chosen the first option, neglecting than the pitch motions, with the only difference that the total weight has been simply divided by four in order to work just with a quarter of the car and obtain directly the values of the stiffness and damper coefficients.

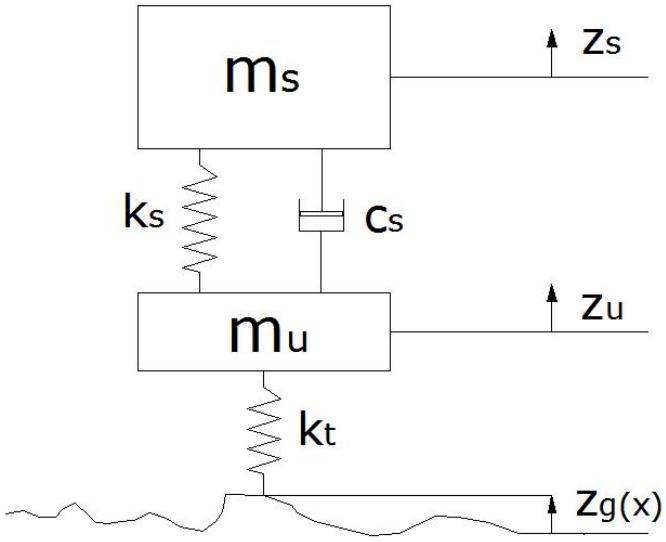

Figure 3.1 – Quarter car model (2dof)

The assumption made in this model are following described:

- all the components have a linear behaviour,
- the vehicle is supposed not to have pitch motion,
- the wheel is supposed not to lose the contact with the ground,

- the ground does not deform.

The coordinate z_u represents the vertical displacement of the wheel centre and z_s is the vertical displacement of a reference point of the chassis, both starting from the static load equilibrium position. This can be done thanks to the hypothesis of linear elastic coefficient. The elastic component k_s and the absorber c_s represent the equivalent spring stiffness and damper coefficient measured at the wheel centre (*wheel rate* and *damper rate*). The equivalent stiffness for example depends both from a and from a :

$$k_s = k_{sp} i_{sp}^2 + \frac{F_z}{i_{sp}} \frac{\mathrm{d}i_{sp}}{\mathrm{d}z_u}, \tag{3.2}$$

The first term is called *geometric term* and depends on i_{sp} (*spring ratio*). It represents the mounting factor between the vertical direction and the real working direction of the elastic element (usually a spring) with stiffness k_{sp}. The second term instead is called *kinematic term* and takes into account how the spring ratio change when there is a variation of geometry due to a vertical external force F_z at the centre of the wheel. Naturally the suspension layout determines the spring ratio i_{sp}. At the moment a layout will be chosen then, the equation (3.2) will need to be used to chose the proper value of the spring stiffness k_{sp}.

The damper rate is defined similarly to the wheel rate but has only a geometric term:

$$c_s = c_{sa} i_{sa}^2, \tag{3.3}$$

where analogously c_{sa} represents the shock absorber damping coefficient and i_{sa} the damper mounting ratio.

The assumption of linear wheel rate and damper rate implies that the vertical displacement are considered to be relatively small remaining in a neighbourhood of the static value where the approximation is still valid.

Finally with k_t is indicated the stiffness of the tyre. Also this component is supposed to have a linear behaviour. For frequencies lower than 30 Hz in fact this assumption is valid. Usually the tyre stiffness is always much greater than the wheel rate with $k_t >> k_S$. It can be interesting to note that the tyre acts like a spring more during rolling than in static condition. That important when the tyre characteristic are measured with a simple static test. The non-rolling stiffness is greater and more non-linear than the rolling stiffness as showed in Fig. 3.2 where an example vertical load deflection relationship is showed, with the curves relative to static conditions and to a travel velocity of 50 km/h.

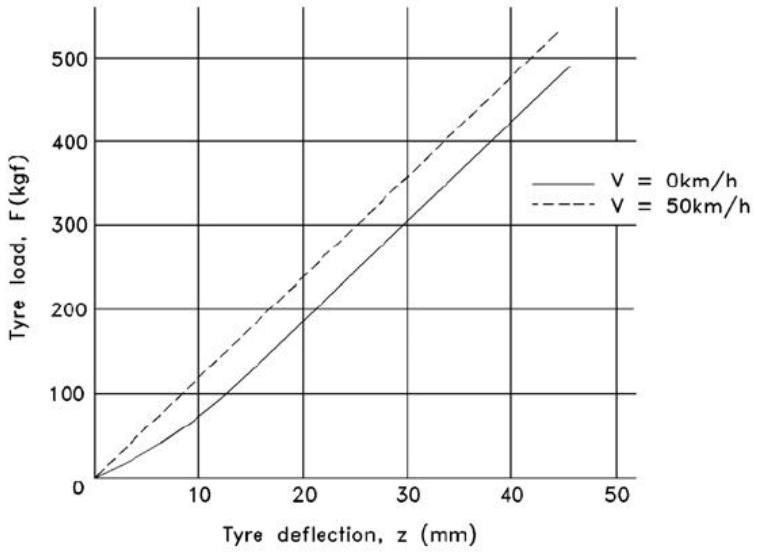

Figure 3.2 – Comparison between "non-rolling" (solid) and "rolling" (dash) tyre stiffness

3.2.1 Equation of motion

Once defined the assumptions it is possible to write the equation of motion of the model.

$$\begin{aligned} &m_s\ddot{z}_s + k_s(z_s - z_u) + c_s(\dot{z}_s - \dot{z}_u) = 0, \\ &m_u\ddot{z}_u + k_s(z_u - z_s) + c_s(\dot{z}_u - \dot{z}_s) + k_t(z_u - z_g) = 0. \end{aligned} \tag{3.4}$$

It is possible to re-write the equations in a more convenient way where it is easier to individuate some suspension characteristic parameter. The following equations are just equivalent at the (3.4)

$$\begin{aligned} \ddot{z}_s &= -2\zeta\omega_s\dot{z}_s - {\omega_s}^2 z_s + 2\zeta\omega_s\dot{z}_u + {\omega_s}^2 z_u, \\ \ddot{z}_u &= -\frac{2\zeta\omega_s}{\mu}\dot{z}_u + \frac{2\zeta\omega_s}{\mu}\dot{z}_s + \frac{{\omega_s}^2}{\mu}z_s - \left(\frac{{\omega_s}^2}{\mu} + {\omega_u}^2\right) z_u + {\omega_u}^2 z_g, \end{aligned} \tag{3.5}$$

where

$$\omega_s = \sqrt{\frac{k_s}{m_s}} \quad \text{rad/s}, \qquad \omega_u = \sqrt{\frac{k_t}{m_u}} \quad \text{rad/s}, \qquad \zeta = \frac{c_s}{2m_s\omega_s}. \tag{3.6}$$

In this form the so called "bounce" and "wheel hop" frequencies are ω_s and ω_u. Naturally they are not the natural frequencies of the system but simple approxi-

mation to them. Also ζ is an approximation of the damping ratio, being the ratio between the equivalent damping coefficient c_s and the critical damping c_{cr} of a single mass system ($c_{\text{cr}} = 2m_s\omega = 2\sqrt{m_s k_s}$). As said before this is only a convenient form to work with and easier to yield results from.

Finally the equations have been manipulate again in order to put them into the state space form:

$$\begin{aligned} \dot{\mathbf{x}} &= \mathbf{A}\mathbf{x} + \mathbf{B}\mathbf{y} \\ \mathbf{y} &= \mathbf{C}\mathbf{x} + \mathbf{D}\mathbf{u} \end{aligned} \tag{3.7}$$

where the system matrices are:

$$\begin{aligned} \mathbf{A} &= \begin{bmatrix} 0 & 1 & 0 & 0 \\ -\omega_s^2 & -2\zeta\omega_s & \omega_s^2 & 2\zeta\omega_s \\ 0 & 0 & 0 & 1 \\ \frac{\omega_s^2}{\mu} & \frac{2\zeta\omega_s}{\mu} & -\left(\frac{\omega_s^2}{\mu} + \omega_u^2\right) & -\frac{2\zeta\omega_s}{\mu} \end{bmatrix}, \qquad \mathbf{B} = \begin{bmatrix} 0 \\ 0 \\ 0 \\ \omega_u^2 \end{bmatrix}, \\ \mathbf{C} &= \begin{bmatrix} -\omega_s^2 & -2\zeta\omega_s & \omega_s^2 & 2\zeta\omega_s \\ \frac{\omega_s^2}{\mu} & \frac{2\zeta\omega_s}{\mu} & -\left(\frac{\omega_s^2}{\mu} + \omega_u^2\right) & -\frac{2\zeta\omega_s}{\mu} \\ 1 & 0 & -1 & 0 \\ 0 & 0 & -1 & 0 \end{bmatrix}, \qquad \mathbf{D} = \begin{bmatrix} 0 \\ \omega_u^2 \\ 0 \\ 1 \end{bmatrix}. \end{aligned} \tag{3.8}$$

The state, input and output vectors instead are defined as follow:

$$\mathbf{x} = \begin{bmatrix} z_s \\ \dot{z}_s \\ z_u \\ \dot{z}_u \end{bmatrix}, \qquad \mathbf{u} = [z_g], \qquad \mathbf{y} = \begin{bmatrix} \ddot{z}_s \\ \ddot{z}_u \\ z_s - z_u \\ z_g - z_u \end{bmatrix}. \tag{3.9}$$

The choice of the output vector $\mathbf{y}$ has been made in order to make some quantities available. In fact the component of the vector $\mathbf{y}$ are all parameters necessary to evaluate the performance of a suspension system. As explained in the previous § 2.4, the main performance criteria of a suspension system are three:

1. the vertical acceleration of the chassis,

2. the suspension working space (or "rattle space"),

3. the variation of contact force between tyre and ground.

So the first and the third component of the vector $\mathbf{y}$ are simply the quantity required by the first two criteria. Regarding the last criterium, the contact force is proportional to the forth component of $\mathbf{y}$, being:

$$F_c = Mg + k_t(z_g - z_u), \tag{3.10}$$

where $g = 9.81$ m/s^2 is the gravitational acceleration and Mg represents the static value for the contact force. Dividing the contact force by the static value it yields

$$\frac{F_c}{Mg} = 1 + \frac{k_t(z_g - z_u)}{Mg} = 1 + \frac{(z_g - z_u)}{\Delta z_u}, \tag{3.11}$$

where Δz_u is the static deflection of the tyre spring. It is clear that if the value expressed by the (3.11) becomes negative the validity of the model is very poor. In fact one of the hypothesis was the wheel never losing contact with the ground. To take into account also this eventuality (that is very common in reality) it would be necessary to develop non-linear model splitting the equations for the two cases. Assuming the force ratio always greater than zero, the performance criterium requires the higher possible value in order to assure the possibility to the shear forces to generate. Naturally this request is less important in a vehicle like *Hyrban* where the maximum velocity is very low and designed only for urban applications.

Finally the second component of the vector $\mathbf{y}$ is the acceleration of the unsprung mass ($\ddot{z}_u$). Naturally it does not represent a comfort parameter but in any case it is an important quantity to analyse when the value of the mass ratio μ increases.

3.2.2 Frequency analysis logic

The quarter car model depicted is a linear system. For this reason it can be applied the "superposition property". Usually this model is studied putting as input a simple harmonic road profile. In this work instead, it has been chosen to put, as input, a random profile ground characterization through its power spectral density (PSD) (see § 2.3.1). In this way the response of the system, that is the vector $\mathbf{y}$, will be in terms of spectral density too. In figure 3.3 this process is schematically showed.

The four transfer functions, $G_i(2\pi f)$, can be easily calculated through the software MatLab. Their are functions of the frequency f. Recalling from the (2.6) the equation of the power spectral density of the road profile in terms of frequency f

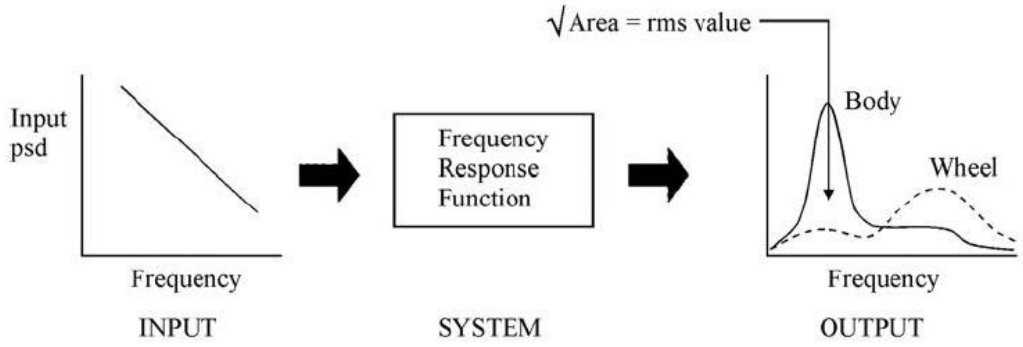

Figure 3.3 – Frequency analysis using PSD

and the velocity v,

$$S_h(f) = \frac{Bv^{(p-1)}}{f^p},$$

it is possible to write the PSD value of the 4 parameter of the vector $\mathbf{y}$ as:

$$S_{\ddot{z}_s} = |G_1(2\pi f)|^2 S_h(f), \tag{3.12}$$

$$S_{\ddot{z}_u} = |G_2(2\pi f)|^2 S_h(f), \tag{3.13}$$

$$S_{(z_s - z_u)} = |G_3(2\pi f)|^2 S_h(f), \tag{3.14}$$

$$S_{(z_g - z_u)} = |G_4(2\pi f)|^2 S_h(f). \tag{3.15}$$

Before the variables will be further manipulated in order to obtain the wanted performance indices ACC, SWS and DTL defined in § 2.4, the first transfer function (3.12) relative to the sprung mass vertical acceleration, needs to be "weighted". This is necessary in order to take into account the different sensitivity of the human body to vibrations as specified by the standard ISO 2631 (1997) (see § 2.3.3. The power spectral density $S_{\ddot{z}_s}$ then, has been multiplied by the frequency filter $W_k(f)$ obtaining a "weighted" psd:

$$\tilde{S}_{\ddot{z}_s} = |G_1(2\pi f)|^2 S_h(f) W_k(f)^2. \tag{3.16}$$

Once obtained the PSD value for all the components of the output vector, the performance indices are defined as the RMS (*Root Mean Square*) of the quantities obtained above. The RMS value of a power spectral density function, calculated in a frequency band (f_1, f_2), is defined as follow:

$$\mathrm{rms}(S(f)) = \sqrt{\int_{f_1}^{f_2} S(f)\,\mathrm{d}f}. \tag{3.17}$$

Subsequently it is easy to define the performance parameters as:

$$\text{ACC} = \text{rms}\Big(\tilde{S}_{\ddot{z}_s}\Big), \tag{3.18}$$

$$\text{SWS} = \text{rms}\big(S_{(z_s - z_u)}\big), \tag{3.19}$$

$$\text{DTL} = \text{rms}\big(S_{(z_g - z_u)} k_t / Mg\big). \tag{3.20}$$

These parameters have been calculated for several value of the mass ratio μ and the damping coefficient c_s.

3.2.3 Stiffness and damping choice

Before proceeding with the analysis and the calculation of the performance indices, it has been necessary to initialize the values of the parameters of model like the suspension equivalent stiffness k_s and the damping coefficient c_s. A first estimation of the value of k_s has been done using the first frequency approximation given by the (3.6). Besides the criterium of Olley are a good reference for the value of the first mode frequency, or better said of the bounce frequency ω_s. Olley was the first man who started studying the problems related with the ride comfort of a vehicle. His first generale criterim says that the bounce frequency of a car should be between 1 and 1.5 Hz. This because the internal organs of the human body have a natural frequency of about 1 Hz and for this reason the man is already used to this frequencies.

In this work it has been chosen to fix the "bounce frequency" at the value of 1.3 Hz for each value of the mass ratio μ:

$$f_s = 2\pi\omega_s = 1.3 \text{ Hz}. \tag{3.21}$$

This choice is a consequence of the sense that takes the mass ratio variation in this work. In fact unlike usual analysis it is not a study of the effect of mounting alloy wheel or not, but it is more a feasibility study on the level of "mass transfer" from sprung to unsprung mass is possible to make. Recalling that ω_s has been defined as an approximation of the first mode frequency it can be written simply as:

$$\omega_s = \sqrt{\frac{k_s}{m_s}} \approx \sqrt{\frac{1}{m_s}\left(\frac{k_t k_s}{k_t + k_s}\right)},$$

where the second approximation is valid as it is always true that $k_t \gg k_s$. It can be easily proven that the values are really close. The choice to fix the bounce frequency

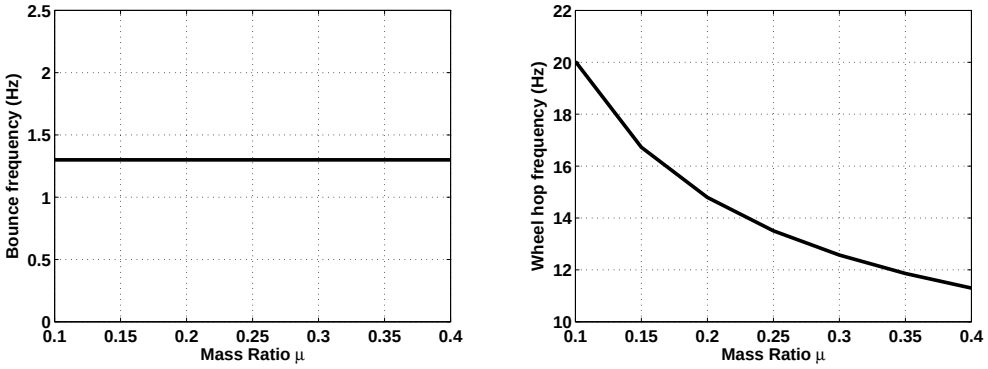

(a) (b)

Figure 3.4 – Bounce and wheel hop frequency variation with the mass ratio μ. ($k_t = 180$ kNs/m, $M = 125$ kg).

yields to a different value of the equivalent suspensions stiffness k_s for each value of the mass ratio μ. This is due to the initial hypothesis to maintain the total mass M constant when μ increase yielding to have $m_s = m_s(\mu)$ and $m_u = m_u(\mu)$.
For this reason then also $k_s = k_s(\mu)$ and its evaluation is

$$k_s = m_s\omega_s^2 = m_s(2\pi f_s)^2 = m_s(2\pi \times 1.3)^2. \tag{3.22}$$

In Fig. 3.5(a) is showed how the equivalent stiffness needs to change to accord the request of a constant bounce frequency ω_s.

The previous figure instead shows the variation of bounce frequency (Fig. 3.4(a)) and wheel hop frequency (Fig. 3.4(b)) with the increasing of the mass ratio μ. Naturally the bounce frequency ω_s is constant as chosen. It can be noticed how the wheel hop frequency decrease very rapidly with the mass ratio.

A good consequence of this choice is that the static load deflection does not vary as the mass ratio μ increase. In fact the static load deflection Δz_s it is given by

$$\Delta z_s = \frac{m_s g(k_s + k_t)}{k_s k_t} + \frac{m_u g}{k_t} \tag{3.23}$$

In Fig. 3.5(b) it is showed how the static load variation remain constant with the change of mass ratio μ thanks to the hypothesis made of constant total mass M. Naturally, according to this procedure, if the value of static deflection will result too high after further consideration (e.g. layout issues, emergency overload, etc.), the suspension would need to be stiffened up with a consequent increasing of the bounce frequency.

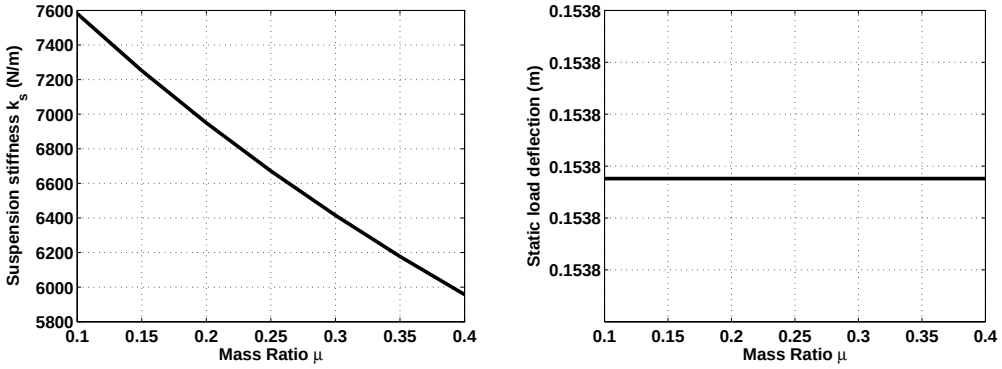

(a) (b)

Figure 3.5 – Variation of the suspension stiffness and static load deflection with the mass ratio μ. ($k_t = 180$ kNs/m, $M = 125$ kg).

Regarding the damping coefficient a common choice in literature is the so called "optimal damping coefficient".

$$c_{s(\text{opt})} = \sqrt{\frac{m_s k_s}{2}}\sqrt{\frac{2k_s + k_t}{k_t}}, \qquad \zeta_{\text{opt}} = \frac{1}{2}\sqrt{\frac{2k_s + k_t}{2k_t}}, \tag{3.24}$$

where ζ_{opt} is conventionally defined as the ratio between the damping coefficient and the critical damping of a single mass-spring system, $c_{cr} = 2\sqrt{m_s k_s} = 2m_s\omega_s^2$.

Equations (3.24) yield from considerations made above the acceleration response function of a quarter car model. Among the curves for several damping coefficients, the one relative to the optimal damping coefficient represents a good compromise between low levels of sprung mass acceleration and uniformity of the response function on the whole frequency spectrum[2].

According to the (3.24) it would seems that the optimal damping coefficient does not depend upon the mass ratio μ. Again this would be true if the hypotheses of keeping constant both the total mass M and bounce frequency ω_s were not valid. So as $m_s = m_s(\mu)$ and $k_s = k_s(\mu)$ also $c_{s(\text{opt})} = c_{s(\text{opt})}(\mu)$ and $\zeta_{\text{opt}} = \zeta_{\text{opt}}(\mu)$. Their behaviour with the mass ratio μ increasing is depicted in Fig. 3.6. If the optimal damping ratio can be considered as almost constant, the optimal damping coefficient is not, having a strong reduction as the mass ratio increase.

For these reasons the simulations have been made for several values of the damping coefficient and not only for the optimal value. Besides

[2]The accurate treatment about the definition and calculation of the optimal damping ratio $c_{s(\text{opt})}$ can be found in [4].

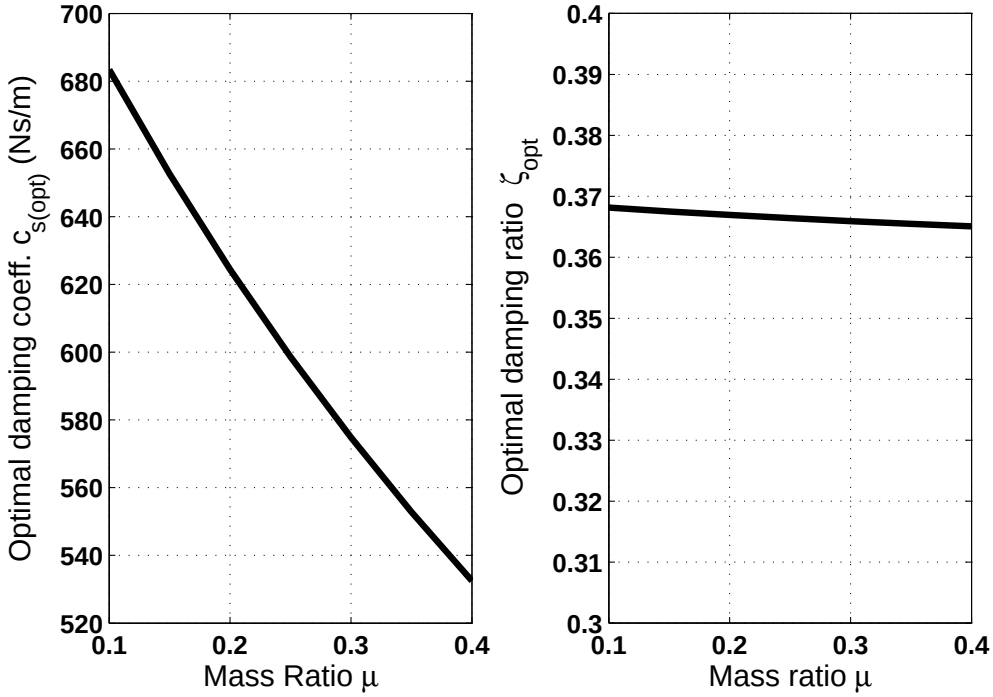

Figure 3.6 – Variation of the optimal damping coefficient $c_{s(\mathrm{opt})}$ and ratio ζ_{opt} with the mass ratio μ.

3.3 Simulations and results

The simulations have been carried out with the software MatLab. The parameters adopted in this study of the quarter car model are showed in the following table.

Parameter	Symbol	Value
Total Mass (1/4)	M	125 kg
Mass Ratio	μ	0.1—0.4
Bounce frequency	ω_s	1.3 Hz
Tyre stiffness	k_t	180 kNs/m
Road unevenness index	B	$5 \cdot 10^{-6}$
Road unevenness coeff.	p	2.5
Velocity	v	20 km/h

Table 3.2 – Simulation parameters

Before calculating the comfort indices, in order to understand immediately the effect of the increasing of the unsprung mass, it is showed, in Fig. 3.7, the graphic with the variation of the transfer function $G_1(2\pi f)$, defined as the ratio between the

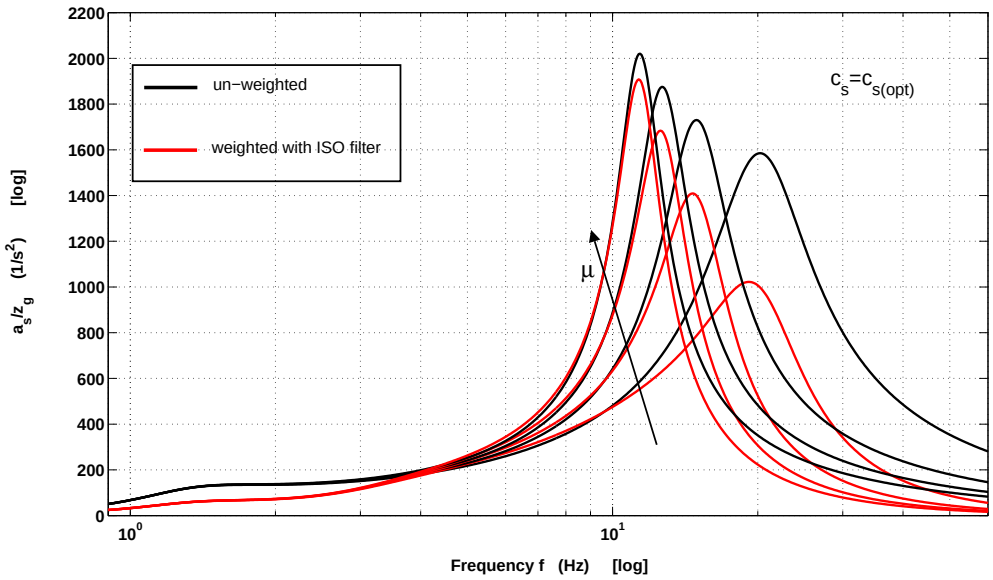

Figure 3.7 – Weighted and unweighted body acceleration transfer function $G_1(2\pi f)$ as the mass ratio μ increases.
(Total mass $M = \text{const} = 125$ kg, $\omega_s = \text{const} = 1.3$ Hz)

body acceleration $\ddot{z}_s$ (or a_s) and the ground input displacement z_g. All the curves are relative to $c_s = c_{s(\text{opt})}$. The transfer function "weighted" with the ISO filter for human sensitivity is showed in red color, while the un-weighted curve is in black.

The previous graphic is the result of the hypotheses described in the previous sections. The following simple observations may be done:

1. The resonance frequency relative to the unsprung mass mode, also called wheel-hop frequency, decreases as the mass ratio μ increase;

2. The maximum value of the acceleration $\ddot{z}_s$ increases with the mass ratio;

3. The resonance frequency relative to the body mode, bounce frequency, is naturally constant (1.3 Hz) because it has been fixed to that value as hypothesis;

4. The acceleration values are relatively with a low total mass M;

5. The human sensitivity filter reduces the maximum acceleration value, but its effects is lower with mass ratio μ increase.

If the first observation it was in such a way expected, the second point is different from what expected. In fact in literature it is verified (see [4]) that the maximum body acceleration value does not vary with the mass ratio. This behaviour is showed

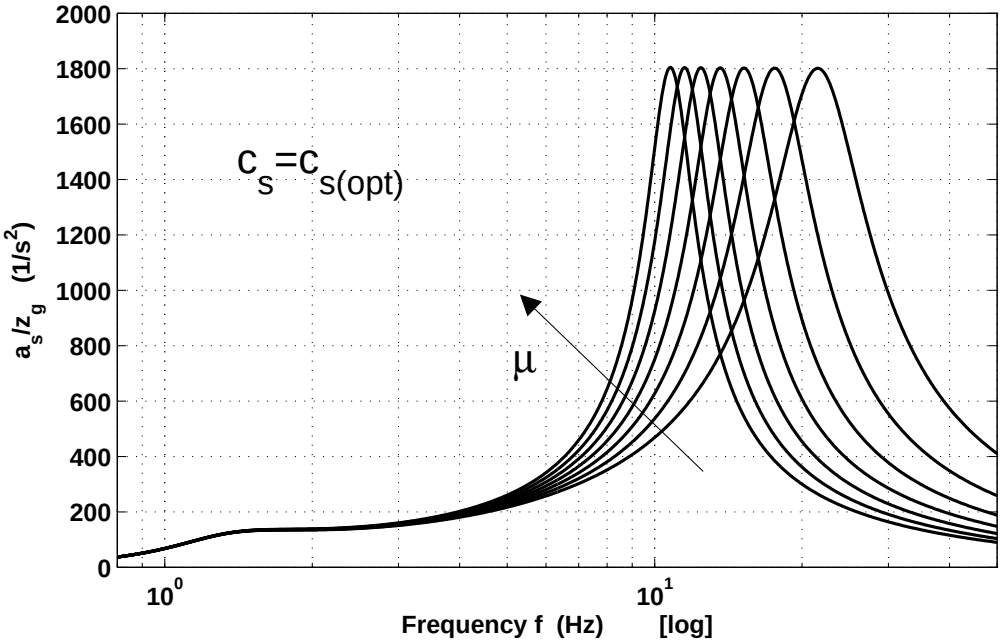

Figure 3.8 – Body acceleration transfer function $G_1(2\pi f)$ as the mass ratio μ increases. (Sprung mass $m_s = \text{const} = 100$ kg, $\omega_s = \text{const} = 1.3$ Hz)

in Fig. 3.8 where it is calculated the transfer function with the same parameters as before but now with no more the hypothesis of constant value for the total mass M, but instead keeping constant the sprung mass m_s. As example it has been used $m_s = 100$ kg. It appears useful to recall that these mass values are relative to a quarter of the vehicle mass. It is clear as now the maximum acceleration remains constant with the mass ratio μ. This result is one of the reasons why it is possible to change the wheel of a vehicle, like putting alloy wheels, without need to change the suspension stiffness. In this work instead, as said before, the aim is more a feasibility preliminary study to understand how much mass can be "transfered" from the sprung to the unsprung mass.

The forth point observed is relative to the high values that the transfer mass assumes, especially for frequency close to wheel-hop frequency. This is due to the small value of the total mass M. In Fig. 3.9 the transfer function G_1 has been calculated for several value of the total mass M in order to underline the effect of having a lightweight vehicle as *Hyrban* car. The curves are all relative to the optimal damping coefficient and with a fixed value of mass ratio $\mu = 0.2$. It may be observed how with a linear decreasing of the total mass, the maximum acceleration increase more than proportionally.

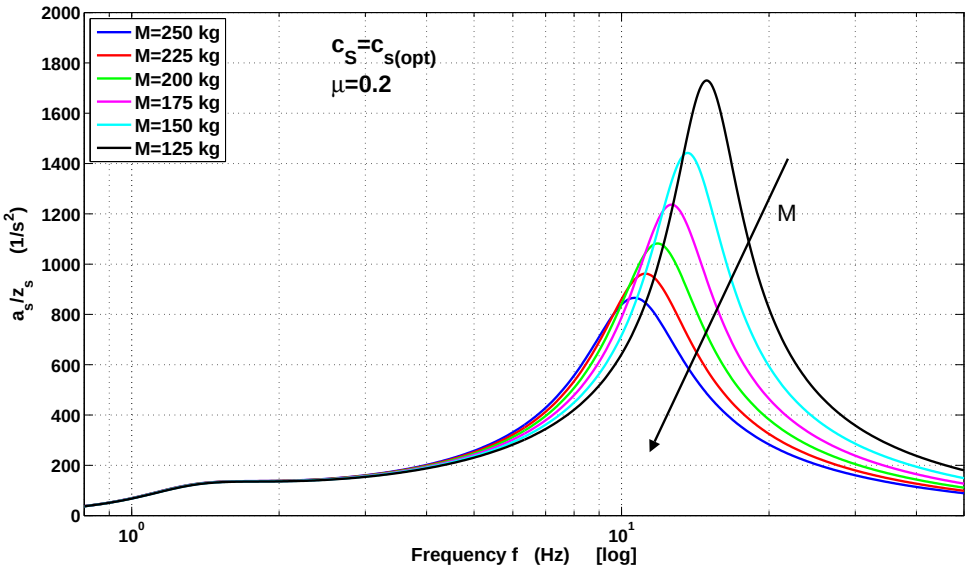

Figure 3.9 – Body acceleration transfer function $G_1(2\pi f)$ as the total mass M decreases. ($\mu = \text{const} = 0.2$, $\omega_s = \text{const} = 1.3$ Hz)

Finally the last point underlines the effect of the ISO weighting filter for human sensitivity. The levels of acceleration are naturally reduced. Even though in Fig. 3.7 it is showed how this reduction effect is smaller as the mass ratio μ increases. For values of μ greater than 0.3 the ISO weighting filter cannot reduced the acceleration peak as it is shifted to lower frequencies where the human sensitivity is bigger.

On the other side, if a small total mass M increases the peak acceleration, it is also true that it shifts to higher values the wheel-hop resonance frequency as can be observed in Fig. 3.9. For the same reason exposed above, this is a positive effect in relation with the ISO weighting filter which has a greater reduction factor for higher frequencies.

Concluding it can be said that the two peculiarity of the *Hyrban* car, lightweight structure and high unsprung-to-sprung mass ratio, are both negative for the comfort of the vehicle. Moreover it has been proven as their effect is more than proportional as, with an high value of μ, not only the peak of the acceleration increases but shifts towards smaller values of frequency where the ISO filter is less effective. A further element that takes part in a bad comfort behaviour is the boundary condition of a constant total mass M, due as said to the limited power availability and to the longitudinal acceleration levels required by the technical specifications.

3.3.1 Performance indices

The observations made so far were made only upon considerations on the transfer function of the system. Then they were relative to a generic harmonic input and it has been discussed just the peak of the response function. Now on the random profile of the road is given as input to the system, in terms of Power Spectral Density (PSD), in order to take into account all the frequencies contained in a typical road. The response functions have been filtered with the ISO weighting function and then a quadratic average (RMS) above frequencies has been done to obtain the comfort performance indices defined before. It is important to underline that the RMS averaging operation and the definition of the comfort parameters as frequency averages takes sense especially from the kind of reaction to vibrations the human body has. In fact a peak of acceleration (if not too high) can be better tolerated than a lower constant acceleration level but lasting for long time. This is clear from the methodology adopted to create the ISO weighting filter explained in § 2.3.3.

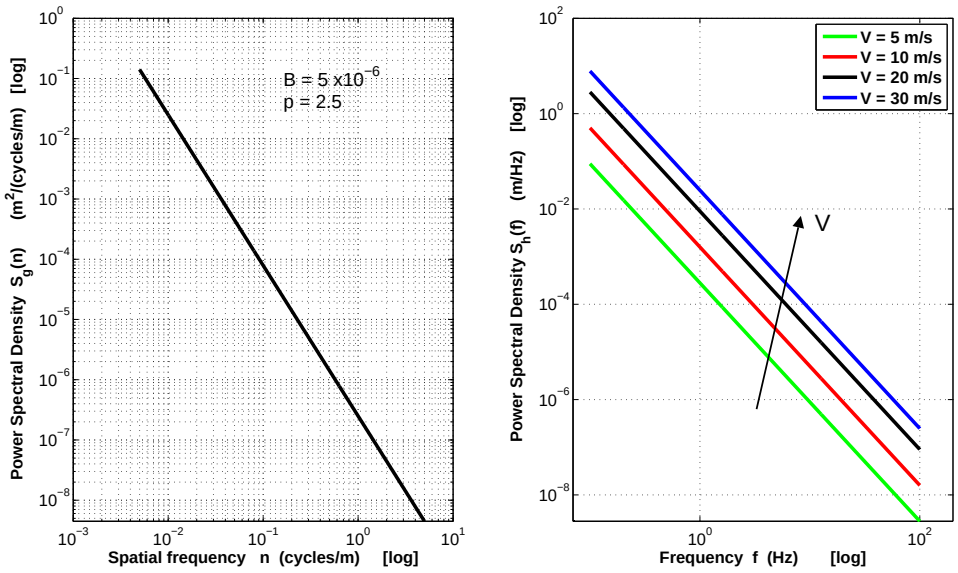

Figure 3.10 – PSD of the road profile elevation in terms of spatial and temporal frequency

The road profile adopted for the simulations is showed in the first graphic of Fig. 3.10 with the unevenness parameters typical of a minor road ($B = 5 \cdot 10^{-6}$ and $p = 2.5$). The representation in term of frequency f shows how increasing the velocity of the vehicle v has the same effect on the spectral profile representation than having a greater unevenness index B.

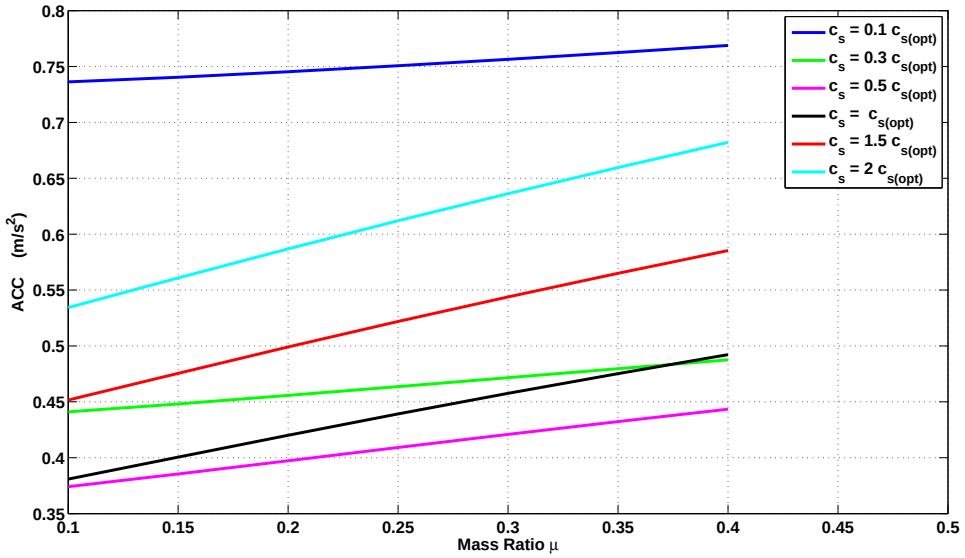

Figure 3.11 – Comfort parameter ACC to mass ratio μ.
(Total mass $M = \text{const} = 125$ kg, $\omega_s = \text{const} = 1.3$ Hz)

The performance indices ACC, SWS and DTL have been calculated for different values of the damper coefficient c_s. In Fig. 3.11 it is showed the variation of the parameter ACC for the mass ratio μ variable from 0.1 to 0.4.

On the results obtained may be done the following considerations:

- For each value of the damping coefficient the parameter ACC increases with the mass ratio μ. This result was expected and confirm how a mass ratio too high reduces the general ride comfort of a vehicle.

- The minimum average value of the curve ACC(μ) is relative to a damping coefficient equal to one half of the optimal one. This results may be used as a first design choice for the shock absorber. Naturally this value would take into account only considerations about comfort and not yet the other performance parameters of a suspension system.

- The curves ACC(μ) have an high average value both for very soft suspension as for hard settings. This results may appear in conflict with the common idea that the softer the suspension the better the ride comfort quality. This behaviour is fundamentally due to the fact that the comfort index ACC represents an average on all the spectrum frequencies neglecting any consideration on the acceleration peak values that may occur for specific damping coefficients at certain frequencies (see Fig. 3.13).

- The slope of the curves ACC(μ) increases with the damping coefficient. This results shows how the ACC parameter is more sensitive to the variation of the mass ratio for high damping values. This results can be important if during the shock absorber design there are also specification of the maximum peak acceleration. This would oblige to adopt an relatively high damping coefficient with consequences when the mass ratio increases.

In order to understand if the previous values of ACC are acceptable, a good reference is given by the standard ISO 2631-1 (1997) that suggests a subjective comfort assessment for several range of ACC values. The table in Fig. 3.12 shows this evaluation.

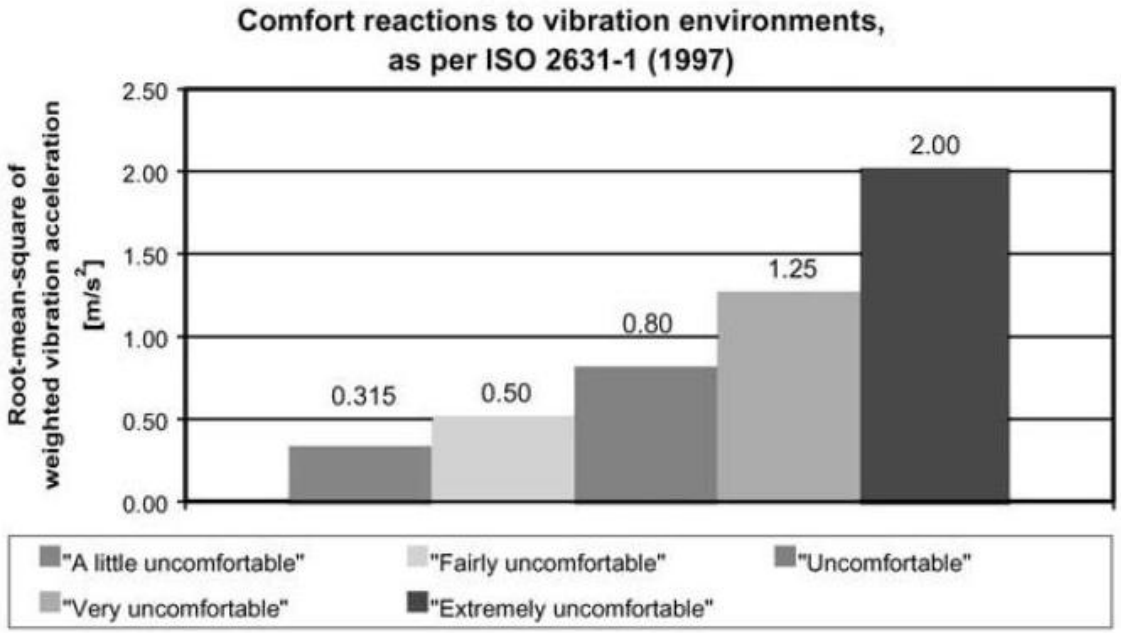

Figure 3.12 – ACC reference values for comfort valuation

Comparing the results obtained in Fig. 3.11 and the reference table it can be concluded that for the parameters of road and velocity adopted the ACC index remains almost constantly in an acceptable zone. This is a good result as the velocity $v = 72$ km/h is almost the maximum velocity allowed and the minor road unevenness coefficients may be considered as a low quality terrain profile.

Going deeper into the third point observation it is useful to present a graphic of the PSD value of the weighted body acceleration for 3 different damping coefficients and for different values of the damping ratio (Fig. 3.13).

Comparing this figure with the ACC curve in Fig. 3.11 is possible to make the following considerations:

1. The maximum PSD value at the wheel hop frequency does not vary much for different values of the damping coefficient;

2. For little mass ratio (i.e. $\mu = 0.1$) the curve relative to $c_s = c_{s(\text{opt})}$ has a peak value (at the bounce frequency) lower than the peak value of the curve relative at $c_s = 0.5c_{s(\text{opt})}$. Even though, according to the graphic in Fig. 3.11 the ACC parameter has a lower average value for $c_s = 0.5c_{s(\text{opt})}$;

3. What observed in the previous point is no more true when the mass ratio is bigger (i.e. $\mu = o.4$) when the peak value is placed at the wheel hop frequency and is roughly the same for each value of the damping coefficient.

The previous observations confirm how a comfort evaluation made considering average indices, as ACC, yields to different conclusions than evaluations made only considering the peak values of the body acceleration. The lat one may be useful when considering a particular road profiles with limited content of frequencies where it is possible to carry out an optimization focused on determined frequencies. But in vehicle design for urban applications it is important to consider all the possible road terrain with a random psd characterization. In this way it is better considered, with the ACC parameter, the long term exposition at vibration considered the acceleration peaks less important for the comfort sensation of the passengers. In any case the peak needs to be evaluated in order not to exceed practical limits.

The curves relative to the indices SWS (Suspension Working Space) and DTL (Dynamic Tyre Load) are following reported in Fig. 3.14 and Fig. 3.15.

Regarding the suspension working space it can be said that its variation with the mass ratio increase is very low. The SWS value then is not sensitive to the unsprung mass ratio. On the other hand it assumes value very different according to the damping coefficient adopted. For suspension very rigid in fact ($c_s \approx 2c_{s(\text{opt})}$) the SWS is very little being about 5 mm. For little damping instead ($c_s \approx 0.1c_{s(\text{opt})}$) the SWS value increase up to 23 mm.

A very important thing to observe is that the SWS parameter (like DTL and ACC) yields from a statistical approach of the road profile modelling. The last can be assumed as a Gaussian random distribution. The response function SWS then is a random distribution as well. In this sense we can affirm to have 68.2%, 95.4% and 99.7% probability that the wheel to body displacement will remain respectively

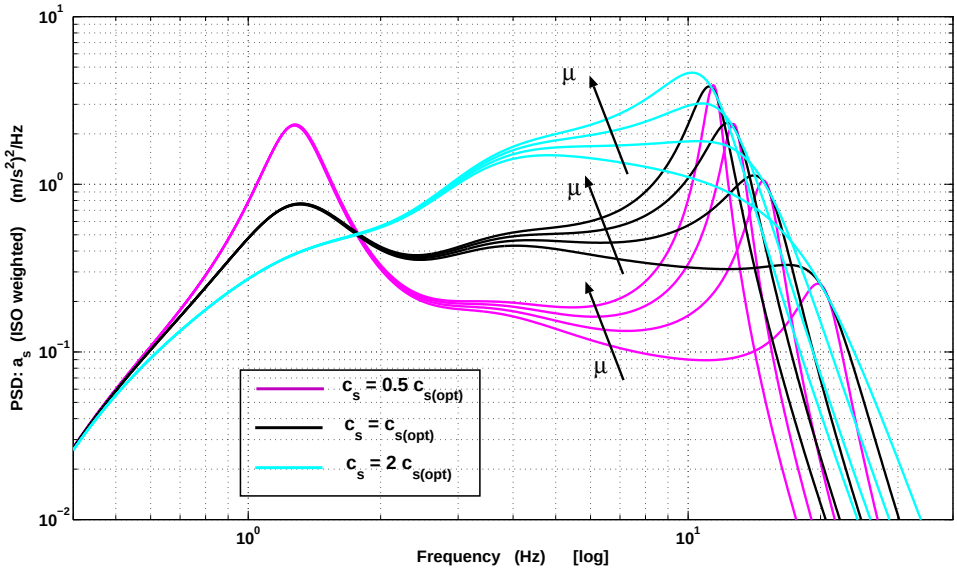

Figure 3.13 – PSD of the body acceleration for different mass ratio μ and damping coefficient c_s.
(Total mass $M = \text{const} = 125$ kg, $\omega_s = \text{const} = 1.3$ Hz)

within ± SWS, ± 2 SWS and ± 3 SWS. In the last case for example for the 0.3% of the time the ends would come into contact. This kind of methodology than can be used when the specification of avoiding bumps hits is strong. In these cases the shock absorber design will start from the SWS parameter keeping it as a boundary condition. In this sense than the SWS parameter assumes a big importance as, being a boundary condition, can influence the optimization of the damping coefficient c_s, affecting then indirectly the level of comfort achievable through the ACC parameter.

In the example studied it has been seen that the best c_s value in terms of ACC parameter was $c_s = 0.5c_{s(\text{opt})}$. For this value the SWS is equal to 10 mm. So with this choice the wheel to body displacement will remain in a neighbourhood of ±3 SWS (60 mm) of its static value for the 99.7 % of the time. If the specification of the vehicle (usually coming from layout issue) are respected it is possible tpo assume this value of the coefficient otherwise it will be necessary to chose an higher damping coefficient with a consequential ride comfort deterioration.

The dynamic tyre load, as said before, is an dimensionless parameter being the ratio between the variation of wheel-road contact force and the static value of this force. Then is preferable its value to be as lower as possible from the unit value, which represents the situation of theoretical lost of contact.

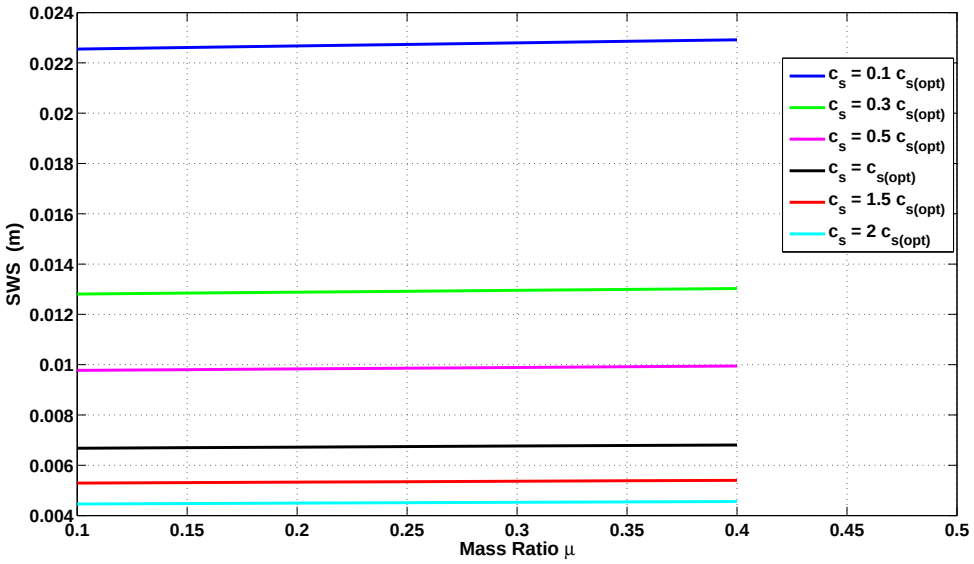

Figure 3.14 – RMS value of suspension working space (SWS) to mass ratio μ.
(Total mass $M = \text{const} = 125$ kg, $\omega_s = \text{const} = 1.3$ Hz)

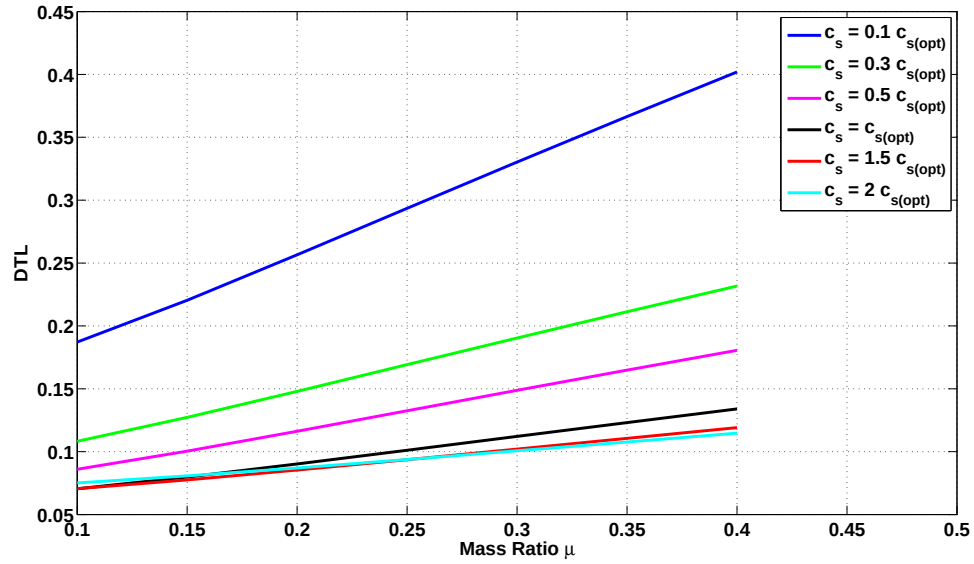

Figure 3.15 – RMS value of dynamic tyre load (DTL) to mass ratio μ.
(Total mass $M = \text{const} = 125$ kg, $\omega_s = \text{const} = 1.3$ Hz)

From the curves showed in Fig. 3.15 it can be noticed that:

- the DTL(μ) average value in μ increases with the reduction of the damping coefficient;
- the DTL(μ) function increase about linearly with the mass ratio μ;
- the sensitivity of the DTL(μ) function to the variation of mass ratio increases with the reduction of the damping coefficient.

What has been said regarding the parameter SWS can be repeated for the parameter DTL. If specifications relative to lateral and longitudinal dynamics performance impose minimum value for the side and braking forces generated in the contact area between tyre and road, this influences the minimum value of DTL acceptable. In this way also DTL can affect indirectly the ride comfort level in the same sense the SWS does.

In the example studied the specification relative to lateral dynamics (*handling*) and longitudinal dynamics (acceleration and braking) are surely less strict than the boundary conditions given from the SWS point of view (layout issues). In fact the velocity of the vehicle is very limited so that the shear force generated when travelling on a bend are usually low. The same thing can be said about the braking forces both because the low velocity and the fact that most of the braking is done by the electric motors working as regenerators and then with transitory braking intervals lower than traditional friction brakes.

Chapter 4

Solutions

In this chapter it is presented a small overview on the possible technical solution to improve comfort are presented. They have been evaluated in terms of possible applicability on the studied *Hyrban* vehicle underlining advantages and disadvantages.

4.1 Comfort optimization issues

In the previous chapter it has been observed how the comfort index, which represents the RMS value of the PSD body acceleration response function, remains within acceptable values for the simulations parameters adopted. Naturally if the same vehicle would travel on a rougher road or with a high velocity also the ACC index would increase. If we consider instead the body acceleration response to single harmonic input signal through its transfer function , it is possible to make considerations above the peak values and not only in terms of comfort index. As example in Fig. 4.1 is reported the "ISO weighted" transfer function relative to a damping coefficient equal to $c_s = 0.5c_{s(\text{opt})}$ at the variation of the mass ratio. It has been proved how this damping coefficient is the first best choice in terms of comfort level ACC.

A conflict could originate if, for instance, is necessary to respect a specification about the maximum peak value and, at the same time, not to reduce the average comfort behaviour, that is given by ACC. The peak acceleration at the wheel-hop frequency, increases with the mass ratio μ. In this case the common solution to increase the damping coefficient would be not inapplicable.

For this reason possible technical solutions available have been qualitatively described. These ideas have not been deeply exploited quantitatively but their possible

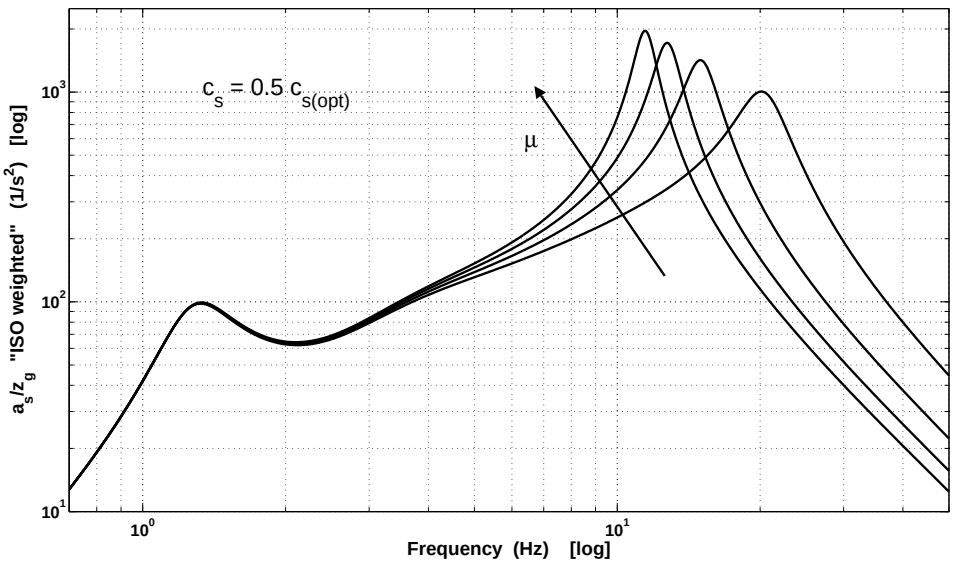

Figure 4.1 – Acceleration of the body a_s for different mass ratio μ

applicability to a vehicle as the *Hyrban* car has been discussed.

4.2 Electric motor and hub decoupling

From the analysis of Fig. 4.1 is clear how the objective would be then to reduce the peak at the wheel-hop frequency. A possibility could be to interpose between the wheel hub and the electric motor another suspension. Considering again a simple quarter car model, this would mean the introduction of another degree of freedom of the system that is the vertical displacement of the motor respect to the body. The electric motor than can be suspended in two different ways:

1. Electric motor suspended to the vehicle body. In this way between the hub and the electric motor there is no elastic reaction but only a rigid kinematic constraint.

2. Electric motor suspended to the hub. In this way the main vehicle suspension is connected with the electric motor, which is suspended to the wheel hub.

The first option is showed schematically in Fig. 4.2 while the second one in Fig. 4.4, both in terms of quarter car modelling. Instead in Fig. 4.3 and Fig. 4.5 a qualitative sketch of the reduction of peak body acceleration is respectively showed for both of the solutions.

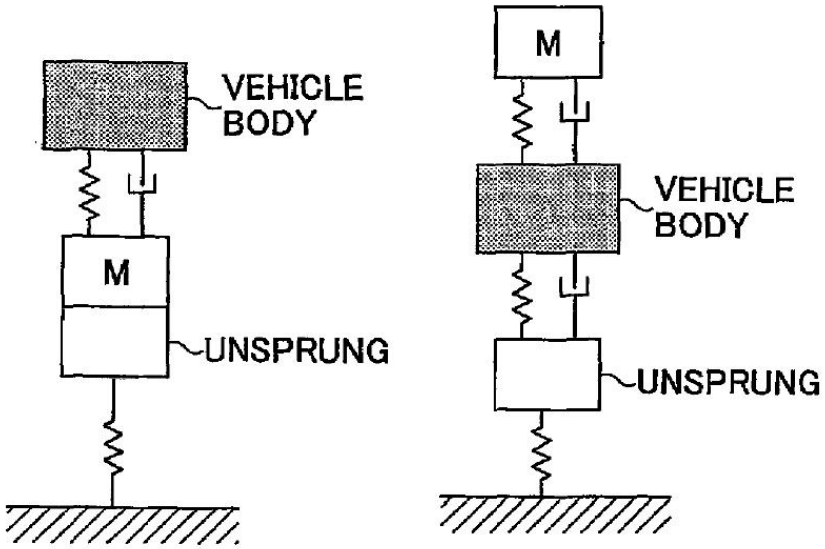

Figure 4.2 – Quarter car scheme of the first decoupling option.

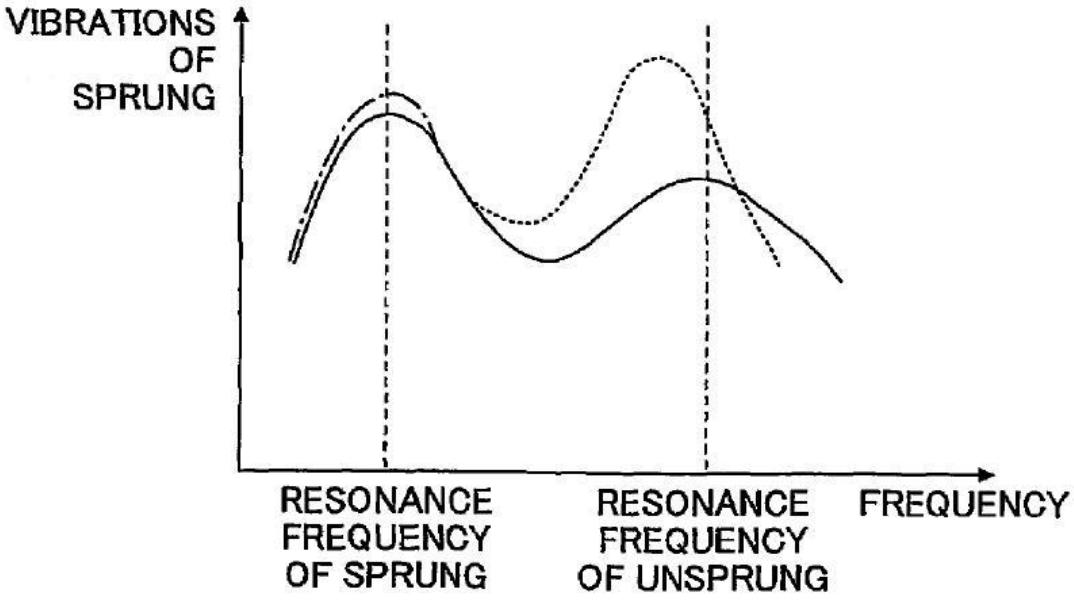

Figure 4.3 – Qualitative variation of the body acceleration response function for the first decoupling option

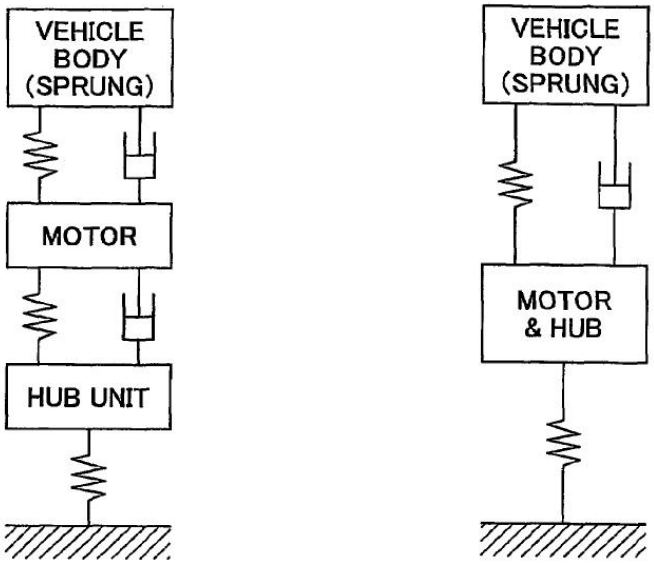

Figure 4.4 – Quarter car scheme of the second decoupling option.

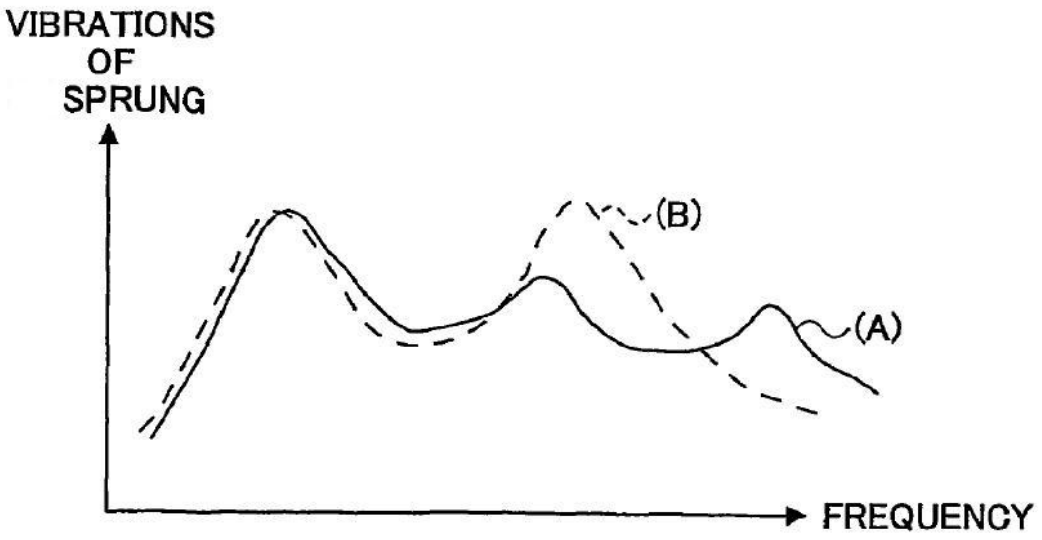

Figure 4.5 – Qualitative variation of the body acceleration response function for the second decoupling option

4.2.1 Technical realisations

US Patent solution

A possible design solution for the decoupling described is showed in Fig. 4.6[1]. The solution is integrated in a McPherson strut suspension system. The rigid kinematic constraint between hub and electric motor has been realized by an omokinetic joint (e.g. *Rzeppa* or *Birfield*). This design scheme is relative to the first decoupling option as can be noticed by the rigid link between the vehicle body and the electric motor.
The advantages of this solution are:

- Reduction of the acceleration peak response;
- Possibility to make the electric motor work as a small dynamic damper for the vehicle body; this can be done for example connecting the fluid chambers of the two shock absorbers (main one and electric motor one) and through a valve regulate the fluid flow in order to obtain the wanted results.

On the other side the disadvantage are:

- Increased total mass of the vehicle caused by the introduction of joint, supports, etc.;
- Reduction of the energy efficiency due to the joint presence;
- The space necessary to the implementation of this solution is much bigger than a compact wheel hub motor.

Analysing pro and contra it appears clear how this kind of solution becomes inapplicable for a vehicle with limited amount of space, energy and with restrictions on total mass like the *Hyrban* car.

Bridgestone solution

The Bridgstone company has proposed instead a technical solution that partially realise the second option decoupling described above. In Fig. 4.7 a sketch of "Bridgestone dynamic-damping in-wheel motor drive system" is showed.

It is possible to note how the electric motor is suspended respect to the hub but not respect to the vehicle body. This means that the idea is the electric motor to

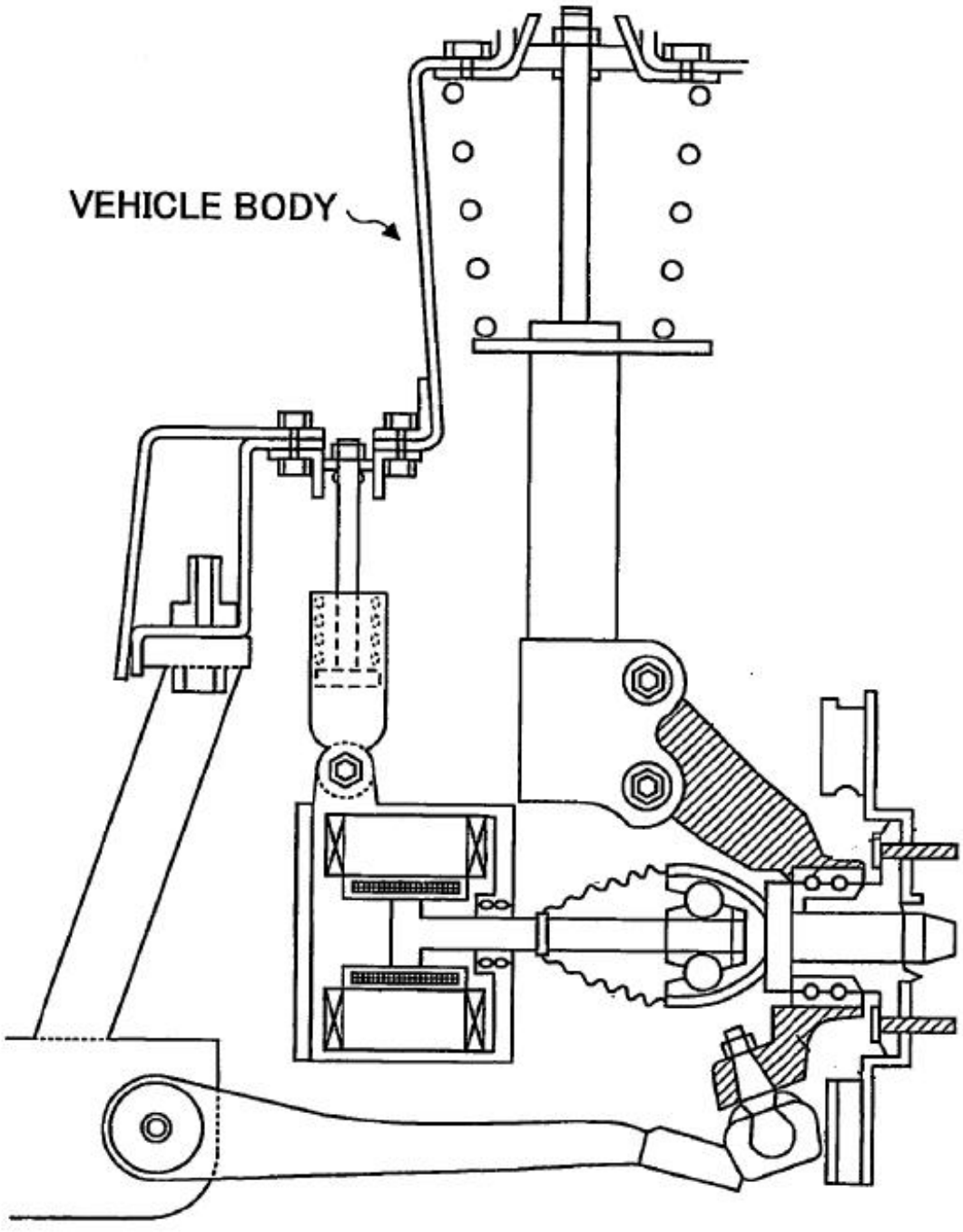

Figure 4.6 – Implementation scheme of the first decoupling option in a McPherson strut suspension.

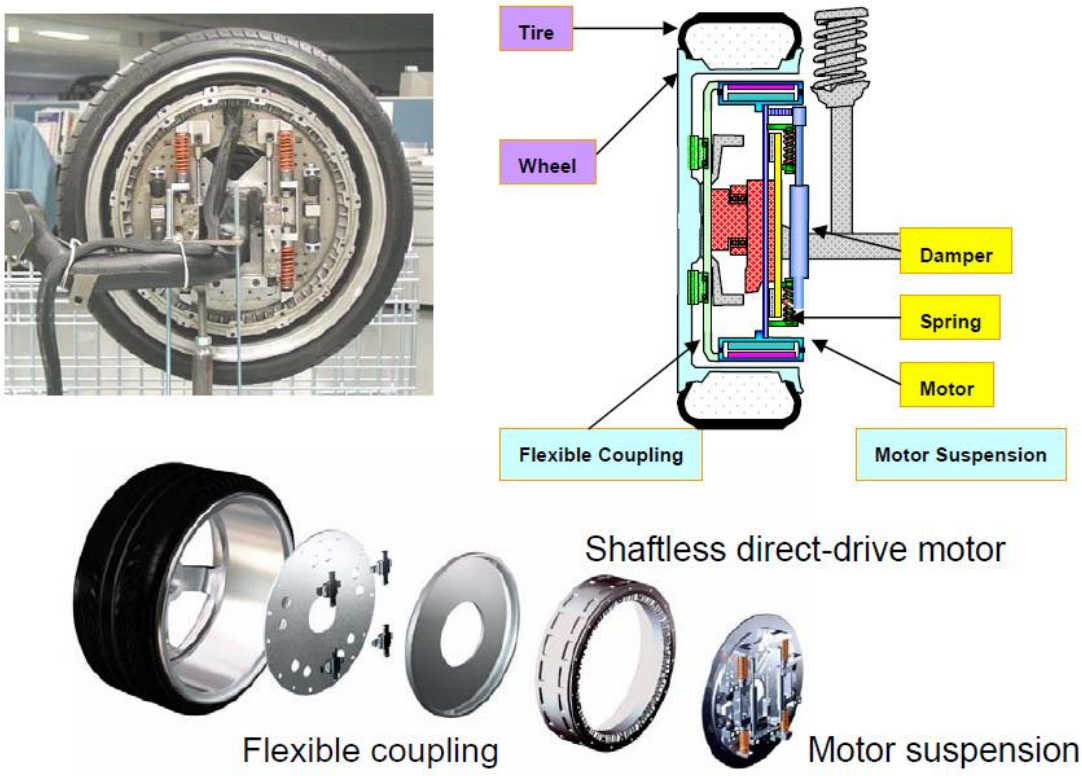

Figure 4.7 – Bridgestone dynamic-damping in-wheel motor drive system

work as dynamic damper for the hub. In this way this influences indirectly the level of vertical vibrations that the hub transmits to the vehicle body.

The structure of the Bridgestone system is fundamentally composed by two elements following described.

Motor suspension. The motor suspension works as a dynamic damper. In fact it suspends the shaftless direct-drive motor to insulted it from the unsprung mass. The motor vibration and the vibration from road and tyres tend to cancel each other, which improves road holding performance.

Flexible coupling. Four cross guides convey the drive power from each motor smoothly to its wheel. The cross guides compensate for the continuous, subtle shifting in the rotation positioning of the motor and wheel.

In order to better understand the potentiality of this system, a series of tests have been conducted by the company. The first test is relative to road-holding capability and consists in monitoring over the time variable the fluctuation of tyre

[1]This design drawing solution has been taken from the US Patent cited in [15].

contact force while the vehicle rolls over a bump on the terrain. The bump is 10 mm high and 20 mm, while the travel velocity is 40 km/h.

The second test conducted instead, is relative to the evaluation of the ride comfort quality. It consists in measuring the body vertical acceleration of an electric vehicle while travelling on a terrain profile having the spectral characteristics of a typical minor road.

The tests have been conducted over three different electric vehicle:

1. traditional electric vehicle equipped with a single motor mounted on the chassis (1);
2. electric vehicle equipped with a conventional in-wheel motor drive (2);
3. electric vehicle equipped with the Bridgestone in-wheel dynamic-damper drive system (3).

The results of the tests described are showed in Fig. 4.8 for the road-holding evaluation and in Fig. 4.9 for the characterization of the ride comfort.

The results shows how the vehicle mounting the dynamic-damper system has a strong reduction of the contact force fluctuation in the time. This means a more uniform contact with better handling properties and less risk of losing grip during cornering, or a quicker return to normal contact force values after hitting an obstacle.

Also the graphics relative to the comfort evaluation, it can be said that there is a net increase of the quality. In fact not only with the dynamic-damping system the peak acceleration in a neighbourhood of the wheel-hop frequency are reduced, but also the peaks are shifted back towards higher frequencies, and then in a less critical zone of road excitation. In fact also in this curve there is the confirmation about how the adoption of in-wheel motors shifted the peak at lower frequency (see curve (1) and (2)). The dynamic system then has the double positive effect of reduction of the peaks and shifting them back to higher frequencies.
Concluding the advantages of this system can be summarized as follow:

- Improved road holding performance and ride quality;
- Compact design;
- Longitudinal comfort, during braking, acceleration and release phases, thank to the flexible coupling guides;
- No power required.

The disadvantages instead are:

- Increase weight;
- Exposition of the system to water and dust;
- Reduced space for the necessary friction brakes;
- Reduced space for steering system.

Evaluating finally the applicability of this solution to the *Hyrban*, it can be said that, in the opinion of the writer, the disadvantages have still a higher weight of the undoubted advantages. In fact if the absence of power requirement represents a big step forward respect the previous solution, it must be said the the excessive weight of this assembly is judged completely not matching with lightweight construction philosophy, distinctive feature of the *Hyrban* car.

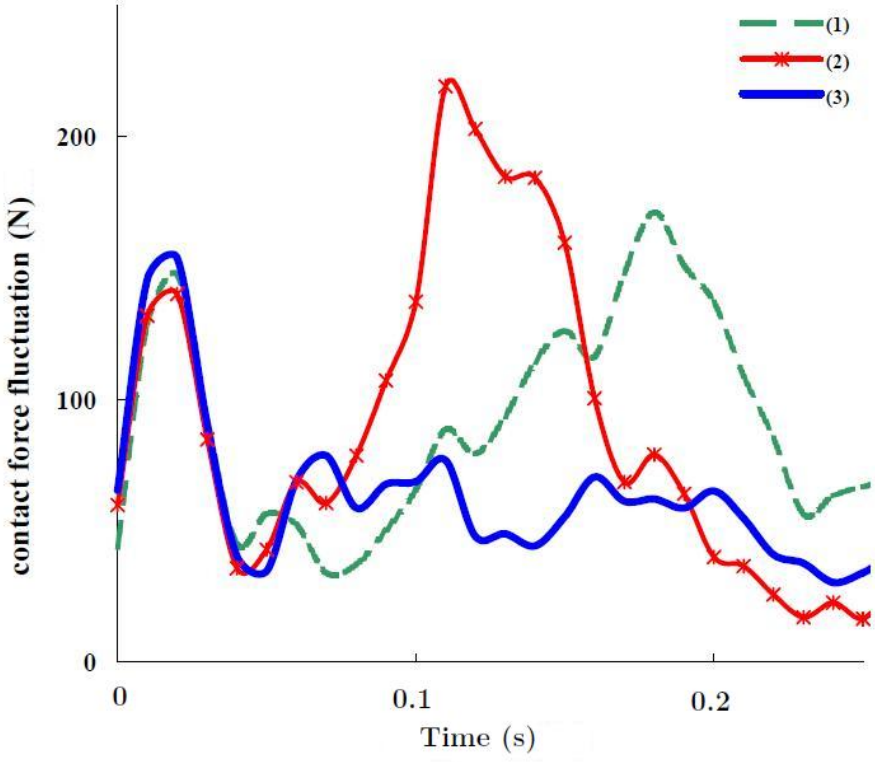

Figure 4.8 – Comparison of tyre contact force fluctuation ΔF_c (N) of a conventional (1), classic in-wheel drive (2) and Bridgestone in-wheel drive (3) electric vehicle.

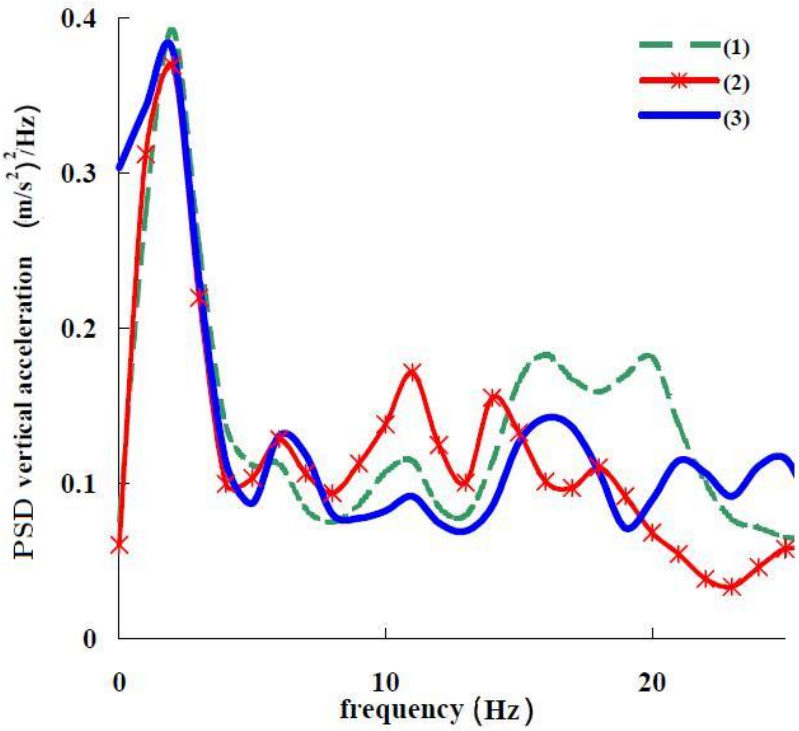

Figure 4.9 – Comparison of the PSD body acceleration of a conventional (1), classic in-wheel drive (2) and Bridgestone in-wheel drive (3) electric vehicle.

4.3 Adjustable dampers

After the short review on the technical possible solutions made in the previous section, it seems useful now to look into solutions relative to different suspension strategies, always remaining in the reference model, which is the quarter car. In §2.5 a quick description of fully active and semi-active systems has already been done. Aim of this section then, is not to evaluate with analytical calculations the effects of any solution, but just give a recommendation on which strategy need to be adopted an optimized.

As a quick example of the motivation for having adjustable dampers is showed in Fig. 4.10 with the "weighted" response function of the body acceleration for different value of the damping coefficient and for a fixed value of the mass ratio $\mu = 0.2$. This graphic shows acceleration as a function of the frequency of a single harmonic input. Considering then not the whole road frequency spectrum input but a single harmonic, it is clear how the best damping option would be to have a different damping coefficient according to the frequency area. A soft damping yields to lower acceleration for most of the spectrum but in the neighbourhood of the resonance frequency the vehicle response changes rapidly.

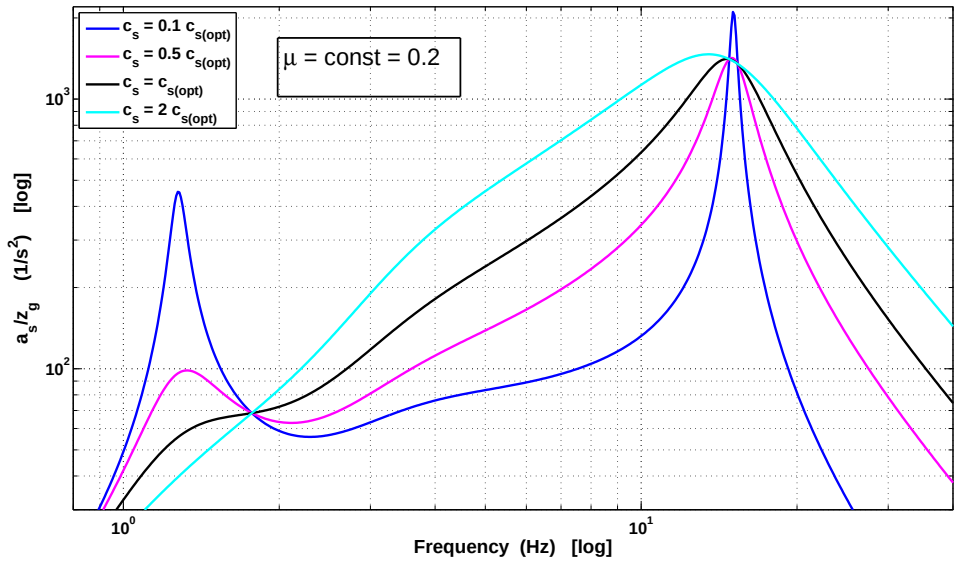

Figure 4.10 – Body acceleration for a fixed value of the mass ratio μ

Analysing the various alternatives adoptable for the case studied, fully active systems are completely excluded from being analysed as possible solution. They are simply not applicable in a vehicle like the *Hyrban* car both because their great

amount of power necessary to work and for the excessive weight. On the other side a possibility seems to be offered by the semi-active suspensions. Their working logic is very similar to the fully active one but with the fundamental difference that they do not input energy but just dissipate it.

4.3.1 Continuously variable dampers

A quarter car representation of semi-active suspension is showed in Fig. 4.11. In this system the actuator present in a possible fully-active suspension, becomes a continuously variable damper mounted in parallel with a conventional spring. The damper is theoretically capable of tracking a force demand signal independently of the velocity across the damper. The demand signal is again generated in a microprocessor according to some control strategy and, like the fully active system, optimal control techniques have been used to derive the control law. However, since this optimal control law cannot be fully implemented because of the non-linear restriction (i.e. it can only dissipate energy and not input it), the system cannot be described as optimally controlled.

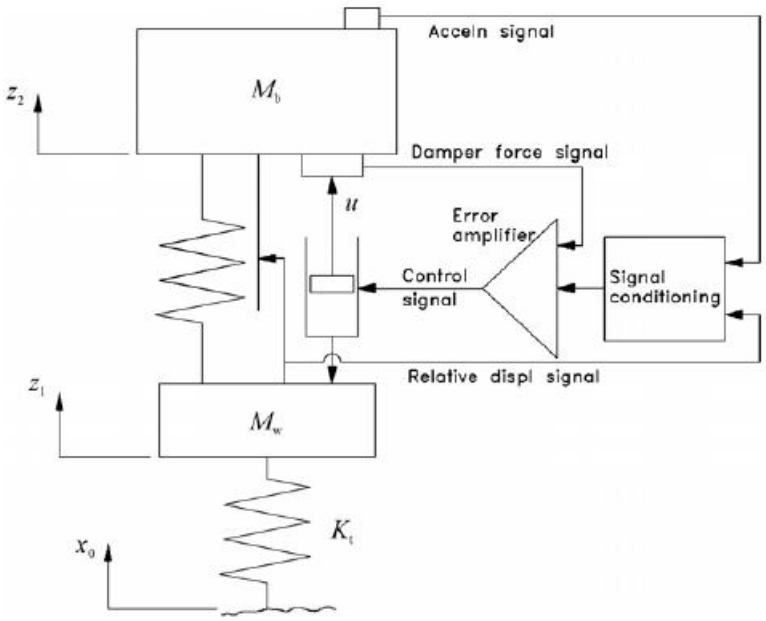

Figure 4.11 – Quarter vehicle model of the semi-active system

In Fig. 4.12 a practical realisation of a continuous damper (a) and a zoom on its electro-valve are showed. Also in this case the final evaluation on the applicability of this system on the *Hyrban* car will need a further analysis when the layout issues, steering system and other design problems will be in a more advanced phase. As a

preliminary study this solution seems to fit with for the vehicle studied. Naturally a control strategy and optimization needs to be carried out as a possible future develpment.

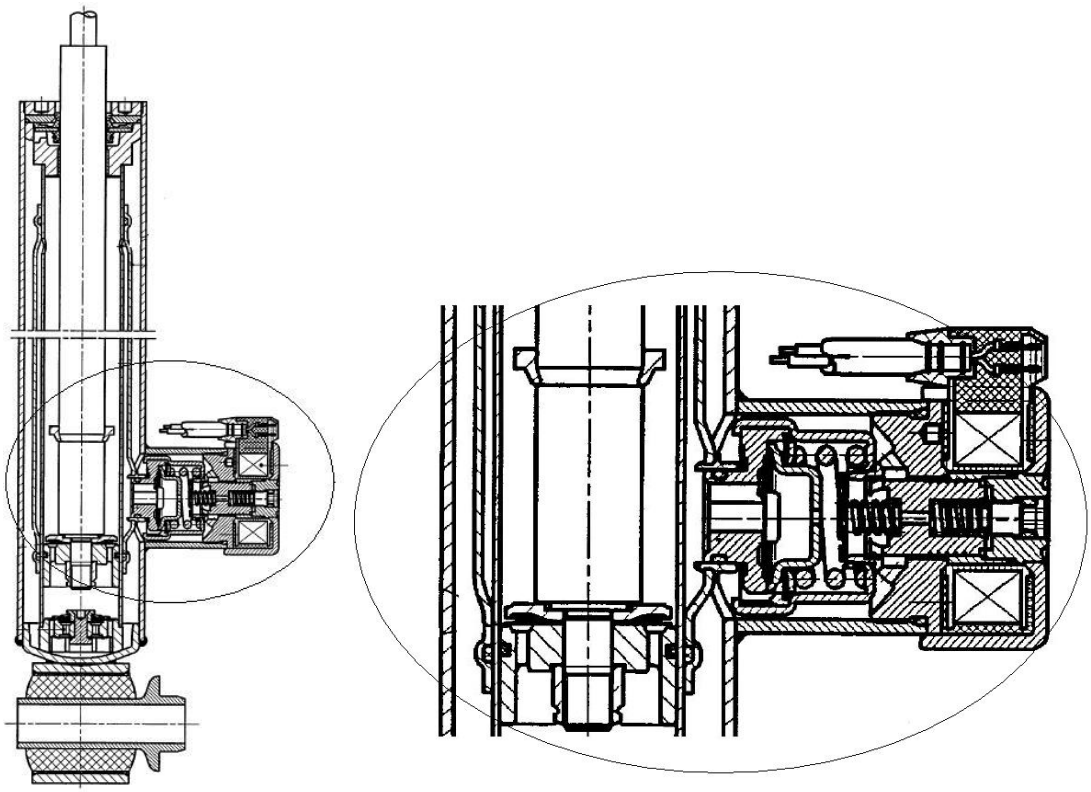

(a) (b)

Figure 4.12 – Continuously variable damper (a) and zoom view of the electro-valve (b).

4.3.2 Switchable dampers

In order to further simplify the suspension system is offered by the switchable dampers. Advanced valves systems can easily "switch" the damper characteristic between 2, 3 or more discrete settings according to the mission. They may be considered as a discrete approximation of continuously variable dampers. For this reason their performance is not comparable with the previous one but the simplicity and the rapid switching between settings (10-20 ms) make then a valid alternative.

Several control law can be adopted. One proposed control law for a two-state damper with hard and soft settings is shown pictorially in Fig. 4.13. The control law relies on the measurement of the absolute and relative body velocities and is

defined by

$$c_s = \begin{cases} c_{\text{hard}} & \text{if} \quad \dot{z}_s \left(\dot{z}_s - \dot{z}_u \right) > 0 \\ c_{\text{soft}} & \text{otherwise} \end{cases} \tag{4.1}$$

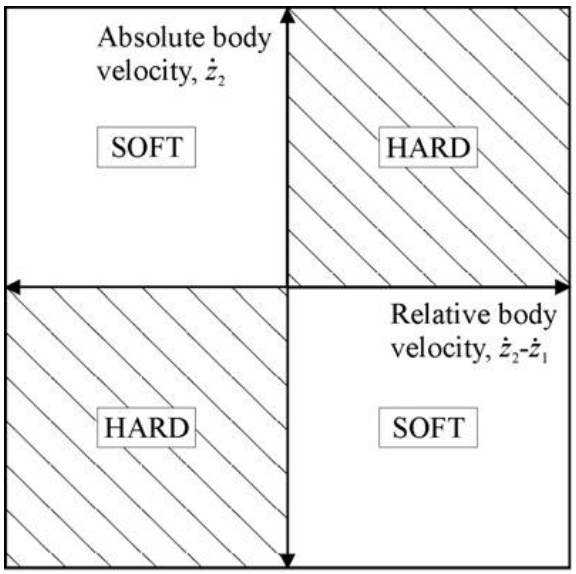

Figure 4.13 – Proposed strategy for two-state switchable damper system

Chapter 5

Conclusions

In the present work the effects on the comfort quality in a fuel cell vehicle of the increased unsprung mass has been studied. A frequency domain analysis of a quarter car model has been conducted. This has been adapted at the specific case studied of the *Hyrban* vehicle through the adoption of working hypotheses as constant total mass value and fixed bounce frequency. They have been defined three performance parameters ACC, SWS and DTL as the rms value respectively of body acceleration, suspension working space and dynamic tyre load. The simulations have been carried out studying the behaviour of the previous parameter when the mass ratio μ increases and using as input to the system a random characterization of the terrain profile of a typical minor road.

The results have showed how all the three parameters degrade with the mass ratio. An interesting observation has been how the peak body acceleration does not remain constant but increase with the mass ratio. This is due to the hypothesis of constant total mass, and then with the consequent idea of mass "transferring" from sprung to unsprung mass. This assumption yielded also the optimal damping coefficient to depend on the mass ratio and not to be constant. Besides according to the ACC comfort evaluation the best damping coefficient is $c_s = 0.5c_{s(\mathrm{opt})}$, and not the common choice of $c_s = c_{s(\mathrm{opt})}$. This is due because the ACC parameter is defined as an average on all the frequency spectrum while the common comfort analysis are made by means of reduction of the peak values. Further it has been observed how ACC is less sensitive to changes of μ when the damping coefficient is lower than the optimal value.

Desiring a good ride behaviour of the vehicle in different conditions without having peaks of the acceleration is necessary the adopt different suspension strategies. Among the various solutions qualitatively analysed, variable dampers and in

particular switchable dampers have been considered as the most appropriate to the *Hyrban* car characteristics, thank to their simplicity, lightness and energy efficiency.

The future developments regard surely the optimization of the switchable damping control law strategy. Besides, even if the maximum vehicle speed is only 80 km/h, the analysis of the lateral dynamics (*handling*) may be an important step forward also for the comfort point of view. For example with the introduction of more complex models (4dof and 7dof) also the pitch and roll motions are considered and their contribution to the passenger comfort may be studied.

Appendix A

Matlab code

```
clear all;format short

%% ISO FILTER %%

load analog_wk


f=logspace(-1,2,1000);   % Temporal frequency (Hz) and
w=2*pi*f;                % Pulsation (rad/s)

[mk,pk]=bode(Wkn,Wkd,w); % ISO filter Bode diagram
mkd=20*log10(mk);        % db

% figure(1),semilogx(f,mkd,'-k','LineWidth',2),...   %ISO filter plot
%   grid on,...
%   xlabel('Frequency [Hz]'),...
%   ylabel('Frequency Weighting [dB]'),...
%   axis([0.01 200 -90 10])
%%  VEHICLE DATA %%


MR=0.10;                     % Mass Ratio
i=1;
while MR<=0.4,
```

```
g=9.81;              % (m/s^2) Gravity acceleration
M=500/4;             % (kg)    Total mass= curb weight (350 kg)
                     %         +2 passengers(150 kg)(4 wheels);
ms=M/(MR+1);         % (kg)    Sprung mass
mu=(MR*M)/(MR+1);    % (kg)    Unsprung mass
ks=ms*(2*pi*1.3)^2;  % (N/m)   Suspension stiffness evaluation
                     %         (first mode frequency 1.3 Hz)
kt=180000;           % (N/m)   Single tyre stiffness
c_ott=sqrt(ms*ks/2)*sqrt((2*ks+kt)/kt);  %Optimal damping coeff.
zita_ott=0.5*sqrt((2*ks+kt)/(2*kt));     %Optimal damping ratio

zita=2*zita_ott;     %         Damping ratio (zita= c/ccrit)

ws=sqrt(ks/ms);      % (rad/s) Bounce radial frequency
wu=sqrt(kt/mu);      % (rad/s) Wheel hop radial frequency
c=2*ms*zita*ws;      % (Ns/m)  Damping Coefficient

%zita=zita_ott;
%c=c_ott;
c_ott_vett(i)=c_ott;
zita_ott_vett(i)=zita_ott;


%% STATE SPACE REPRESENTATION%%

A=[0 1 0 0;-ws^2 -2*zita*ws ws^2 2*zita*ws;0 0 0 1;...
    (ws^2)/MR (2*zita*ws)/MR -(((ws^2)/MR)+wu^2)...
    -(2*zita*ws)/MR];
B=[0 0 0 wu^2]';
C=[-ws^2 -2*zita*ws ws^2 2*zita*ws;...
    (ws^2)/MR (2*zita*ws)/MR -(((ws^2)/MR)+wu^2)...
    -(2*zita*ws)/MR;1 0 -1 0; 0 0 -1 0];
D=[0 wu^2 0 1]';
twodof=ss(A,B,C,D);
```

```
    [m,p]=bode(twodof,w);
    m=squeeze(m);
    p=squeeze(p);

    md=20*log10(m);

    %figure(1),semilogx(f,md,'k'),grid on
    %figure(2),semilogx(f,p,'k'),grid on



%% ROAD PROFILE CHARACTERIZATION %%


    U=20;                   % (m/s) Velocity

    B=5*1e-6;      %'k'     % Unevenness index
    %B=3*1e-5;     %'r'
    %B=1e-5;       %'b'
    n=2.5;                  % Unevenness coeff.


    phi=f/U;                % (cycle/m) Spatial frequency

    Szgs=B*phi.^-n;         % m2/(cyc/m)
                            % psd profilo stradale rispetto
                            % alla frequenza spaziale
    Szg=Szgs/U;             % m2/Hz
                            % psd profilo stradale rispetto
                            % frequenza temporale

    figure(3),subplot(1,2,1),loglog(phi,Szg,'k'),...
      axis([0.001 10 0 1]),grid on;hold on
    figure(3),subplot(1,2,2),loglog(f,Szgs,'b'),....
      axis([0.3 40 0 100]),grid on;hold on
    legend(axes1,{'data3','data6','data9','data12'},...
```

```
        'FontSize',12,'FontWeight','demi');


%% ACC %%

    AsZg=m(1,:);                    %funz trasferimento
                                    %accelerazione massa sospesa
      AsZgw=AsZg.*mk';
    % figure(4),semilogx(f,AsZg,'k','LineWidth',2),...
    % axis([0.8 50 0 2200]),grid on,hold on
    % figure(4),semilogx(f,AsZgw,'r'),grid on,hold on
    ZsZg=AsZg./(w.^2);              %funz spostamento massa sospesa

    % figure(5),semilogx(f,20*log10(ZsZg),'r'),grid on


    SAs=Szg.*AsZg.^2;     % psd accel massa sospesa
    SAsw=SAs.*mk'.^2;     % psd accel massa sospesa PONDERATA
                          % con filtro ISO
    % figure(6),loglog(f,SAs,'k'),axis([0.3 40 -1 10]),...
     % grid on,hold on;
    % figure(6),loglog(f,SAsw,'k'),grid on,hold on;

    df=f(2)-f(1);

    msAs=sum(SAs)*df;
    msAsw=sum(SAsw)*df;

    rmsAs=sqrt(msAs);         % ACC non ponderato
    rmsAsw=sqrt(msAsw);       % ACC ponderato

    rmsAs_vett(i)=rmsAs;      %vettore ACC non ponderato
                              %al variare di MR
    rmsAsw_vett(i)=rmsAsw;    %vettore ACC ponderato
                              %al variare di MR
```

```
    ACC=rmsAs;
    ACC_vett(i)=ACC;

    ACCw=rmsAsw;
    ACCw_vett(i)=ACCw;

%% SWS (Suspension Working Space) %%

    CaZg=m(3,:);      %funz trasferimento (zs-zu)
                      %(differenza cassa-assale (Ca) rispetto
                      % ingresso profilo (Zg)
    SCa=Szg.*CaZg.^2; %psd Cassa-assale
    msCa=sum(SCa)*df;
    rmsCa=sqrt(msCa);        %SWS
    rmsCa_vett(i)=rmsCa;     %vettore valori SWS al variare di MR
    SWS=rmsCa;
    SWS_vett(i)=SWS;



%% DTL (Dynamic Tyre Load) %%

    PaZg=m(4,:);           % funz trasferimento (zg-zu)
                           % (differenza profilo-assale (Pa))
                           % rispetto ingresso profilo Zg
   % FcZg=(PaZg*kt)./(M*g); % funz trasferimento rapporto
                           forza contatto profilo-ruota (Fc)su peso
                           statico rispetto ingresso profilo Zg

   % figure(12),semilogx(f,FcZg,'r'),grid on,hold on
   % figure(12),semilogx(f,PaZg,'g'),grid on,hold on
    SPa=Szg.*PaZg.^2;
    msPa=sum(SPa)*df;
    rmsPa=sqrt(msPa);
    rmsPa_vett(i)=rmsPa;
```

```
    DTL=(rmsPa)*(kt/(M*g));  %DTL
    DTL_vett(i)=DTL;         %Vettore valori DTL al variare di MR


%%

    MR=MR+0.05;
    % MR=MR+0.1;
    i=i+1;

end
    % MR=0.10:0.1:0.4;
    MR=0.10:0.05:0.4;


%% PLOTS %%


    % figure(8),plot(MR,ACC_vett,'g--'),grid on,hold on
    % figure(8),plot(MR,ACCw_vett,'c'),grid on,hold on
      % rmsAsdiff_vett=rmsAs-rmsAsw_vett;
      % figure(8),plot(MR,rmsAsdiff_vett,'g'),grid on
    % figure(9),plot(MR,SWS_vett,'r'),grid on
    % figure(10),plot(MR,DTL_vett,'c'),grid on,hold on
    % figure(11),subplot(1,2,1),plot(MR,c_ott_vett,'r',...
    % 'LineWidth',2),grid;axis([0.1 0.4 520 700]),...
    %     xlabel('\mu'),ylabel('Coeff. smorzamento ott. c_s (Ns/m)');
    % figure(11),subplot(1,2,2),plot(MR,zita_ott_vett,'b',...
    % 'LineWidth',2),grid;,xlabel('Mass ratio \mu'),ylabel...
    % ('Fattore di smorzamento ott.\zeta_{opt}');
```

Bibliography

[1] Cavallo, A., Setola R. and Vasca, F. (2002). *La nuova guida a Matlab, Simulink e Control Toolbox*. Liguori Editore.

[2] Crolla, D.A. (1996). *Vehicle dynamics – Theory into practice*. Proc. IMechE Part D, Journal of Automobile Engineering, **210**, D2, 83–94. [1995 Automobile Division Chairman's Address]

[3] Crolla, D.A. (2005). *Vehicle Dynamics Lectures Notes*. Cranfield University, School of Mechanical Engineering, UK.

[4] Guiggiani, M. (2007). *Dinamica del veicolo*. 2nd ed., CittàStudiEdizioni, Torino.

[5] Jorgensen, K. (2008). *Technologies for electric, hybrid and hydrogen vehicles: electricity from renewable energy sources in transport*. Utilities Policy, **16**, 72–79.

[6] Michelin (2002). *The Tyre: Comfort*. CD, Société de Technologie Michelin, Clermont-Ferrand.

[7] Meirovitch, L. (1986). *Elements of Vibration Analysis*. 2nd ed., McGraw Hill, New York.

[8] Miller, L.R. (1988). *Tuning passive, semi-active, and fully active suspension systems.* Proceedings of the 27th IEEE Conference on Decision and Control, **3**, 2047–2053.

[9] Purdy, D.J. and Simner, D. (2004). *A brief investigation into the effect on suspension motions of high unsprung mass*. Journal of Battlefield Technology, **7**, No. 1.

[10] Robson, J.D. (1979). *Road surface description and vehicle response*. International Journal of Vehicle Design, **1**, No.1.

[11] Schmitt, P. (2007). *Just build it! A fully functional concept vehicle using robotic wheels.* Master of Sciences Thesis, Massachusetts Institute of Technology.

[12] Sharp, R.S. and Crolla, D.A. (1987). *Road vehicle suspension system design – a review.* Vehicle System Dynamics, **16**, 167–192.

[13] Spowers, H. (2006). *A whole system design approach to personal transport.* IABSE Henderson Colloquium, Cambridge, 10–12 July 2006.

[14] Standard ISO 2631-1 (1997). *Mechanical vibration and shock — Evaluation of human exposure to whole-body vibration. Part 1: General requirements.*

[15] U.S.Patent 7413203 B2. *Suspension system for electric vehicle.* Fumito Kurata, Toyota (JP).